Corrosion Science 108 (2016) 94–110

Contents lists available at ScienceDirect

Corrosion Science

journal homepage: www.elsevier.com/locate/corsci

Empirical and quantum chemical studies on the corrosion inhibition performance of some novel synthesized cationic gemini surfactants on carbon steel pipelines in acid pickling processes

Hany M. Abd El-Lateef[a,*], Mohamed A. Abo-Riya[b], Ahmed H. Tantawy[b]

[a] Chemistry Department, Faculty of Science, Sohag University, 82524 Sohag, Egypt
[b] Chemistry Department, Faculty of science, Benha University, 13518 Benha, Egypt

ARTICLE INFO

Article history:
Received 13 January 2016
Received in revised form 7 March 2016
Accepted 8 March 2016
Available online 11 March 2016

Keywords:
A. Acid solutions
A. Carbon steel
B. EIS
B. SEM
B. Polarization
C. Acid inhibition

ABSTRACT

Three novel cationic gemini surfactants were synthesized and their effect on the corrosion of carbon steel in 15% HCl solution was investigated using weight loss, electrochemical impedance spectroscopy, potentiodynamic polarization, surface analysis (SEM and EDX) and quantum chemical methods. The surface parameters of the synthesized surfactants were calculated from the surface tension and conductivity measurements The results revealed that the prepared surfactants were effectively inhibited the carbon steel corrosion in 15% HCl. Analysis of polarization data indicates that all surfactants act as mixed type inhibitors. The inhibitors adsorption on the metal surface obeyed Langmuir isotherm. The correlation between empirical and theoretical results was discussed.

© 2016 Elsevier Ltd. All rights reserved.

1. Introduction

Carbon steel is the most widely used engineering materials including marine applications, metal-processing equipment, nuclear plants, transportation, pipelines, mining, chemical processing and construction [1–4]. It is usually exposed to strong acids particularly HCl solutions between 5 and 15% at temperature range 60–80 °C in operations like industrial acid improvement, acid pickling processes, acid descaling and oil well acidizing [5,6]. With a view to decrease the acid corrosion to carbon steel pipeline, inhibitors are utilized as an effective and economical process. Most of the used efficient inhibitors contain heteroatom like nitrogen, oxygen, sulfur and multiple bonds in their molecules through which they can be adsorbed on the electrode surface [7–9]. Their inhibition performance can be affected by varieties of factors, such as temperature of the medium [10], metallic kind [11], corrosive environments [12] and the molecular structure of the studied inhibitor [13].

An important corrosion inhibition tool is the use of surfactant inhibitors. This is attributed to their significant ability to influence the properties of surfaces and interfaces. The most important action of inhibition is the adsorption of the surfactant functional group onto the metal surface [14], adsorption is critical to corrosion inhibition. The ability of a surfactant molecule to adsorb is usually due to its capability to aggregate to form micelles. The adsorbed molecules form a monolayer or bilayer, admicelles or hemimicelles and prohibit the acids to attack the metal surface, and thus reduce the corrosion.

Recently, gemini surfactants have been developed as a new generation of surfactants [15]. This kind of surfactant consists of two classical surfactant molecules chemically bonded together by flexible or rigid spacer [16]. These surfactants have superior surface activity, surface properties, very low critical micelle concentration (CMC) and high solubilising capacity at low concentrations than corresponding conventional surfactants [17]. While the environmental considerations have the global concern now, the scientists interested in solving this problem. One of these solutions is to prepare cationic gemini surfactants with readily labile groups such as ester or amide group [18]. Gemini surfactants as corrosion inhibitors for carbon steel pipelines in acidic media have been studied [19–21]. Research activities in present cases are geared towards developing the non-toxic, cheap and environment friendly corrosion inhibitors. Quantum chemical calculations are being used to investigate the corrosion inhibition mechanism [22,23]. In addition, theoretical calculation can provide insights into the correlation of

* Corresponding author.
E-mail addresses: Hany_shubra@yahoo.co.uk, Dr_hanycorr@hotmail.com (H.M. Abd El-Lateef).

http://dx.doi.org/10.1016/j.corsci.2016.03.004
0010-938X/© 2016 Elsevier Ltd. All rights reserved.

the electronic properties and the corrosion inhibition performance [24].

The main objective of the current investigation was to synthesis and evaluate three novel cationic gemini surfactants with an ester linkage as corrosion inhibitors in carbon steel/surfactnt/15% HCl solution system by means of weight loss measurements, electrochemical techniques (potentiodynamic polarization and electrochemical impedance spectroscopy measurements), surface tension, conductivity measurements, biodegradability, surface analysis (scanning electron microscopic and energy dispersive X-ray spectroscopy (SEM/EDX)) and theoretical calculation methods. Adsorption thermodynamic parameters are calculated and discussed in detail. Besides, an effort is made to illustrate the mechanism of corrosion inhibition.

2. Material and Methods

2.1. Materials

Octan-1-amine (97%), dodecan-1-amine (97%), and hexadecan-1-amine (98%) were obtained from Acros organics company (Belgium) and used without further purification. 2-Chloroacetyl chloride (97%) and cyclohexane-1,4-diol (99%), were purchased from Aldrich company. Acetonitrile (99%), diethylether (99%), K_2CO_3 (anhydrous), dimethylformamide (DMF, 97%), triethylamine (97%), and dimethyl sulphate (98%), were obtained from AL-Nasr chemical company.

Carbon steel electrode with composition (w%) C 0.16%, Si 0.18%, Ni 0.01%, Mn 0.71%, S 0.04%,Cr 0.01% and remainder Fe was used for the electrochemical studies.

The corrosive solution (15% HCl) was prepared by dilution of AR grade HCl with bidistilled water. The volume of acid solution was 500 mL. The concentration range of inhibitors employed was 25–200 ppm by weight.

2.2. Methods

2.2.1. Synthesis of the cyclohexane cationic gemini surfactants

The studied inhibitors, namely, *N,N'*-((cyclohexane-1,4-diylbis(oxy))bis(2-oxoethane-2,1-diyl))bis(*N,N*-dimethyloctan-1-aminium) methyl sulfate (CHOGS-8), *N,N'*-((cyclohexane-1,4-diylbis(oxy))bis(2-oxoethane-2,1-diyl))bis(*N,N*-dimethyldodecan-1-aminium) methyl sulfate (CHOGS-12) and *N,N'*-((cyclohexane-1,4-diylbis(oxy))bis(2-oxoethane-2,1-diyl))bis(*N,N*-dimethylhexadecan-1-aminium) methyl sulfate (CHOGS-16) were prepared in three steps, as shown in Fig. 1.

2.2.1.1. Synthesis of cyclohexane-1,4-diyl bis(2-chloroacetate) [compound II]. 2-Chloroacetyl chloride (3.86 g, 35 mmol) was placed in 100 mL round- bottom flask with a magnetic bar in an ice-water bath with continuous stirring. Triethylamine (4 g, 35 mmol), cyclohexane-1,4-diol (2 g, 17 mmol) and dichloromethane (20 mL) was slowly added over 10 min in ice bath with a constant pressure dropping funnel. The mixture was stirred for 6 h at room temperature. The solvent was then evaporated by rotary evaporator and white solid powder was obtained. The solid was washed several times with bidistilled water and recrystallized from ethanol to give the desired product as a white powder in 95% yield.

2.2.1.2. Synthesis of cyclohexane-1,4-diyl bis(2-(alkylamino) acetate [compound III]. Different alkan-1-amines (octan-1-amine, dodecan-1-amine and hexadecan-1-amine) (7.4 mmol) in 50 mL acetonitrile was added separately to a solution of compound **II** (1 g, 3.7 mmol) in 25 mL acetonitrile in a round-bottomed flask (100 mL). The mixture was maintained at 80 °C and pH = 9 (by adding 10% K_2CO_3) for 6 h. After the reaction was completed, the mixture was filtered. The solvent was removed and the solid product was washed several times and crystallized from ethanol to give the desired product in 85% yield.

2.2.1.3. Synthesis of N,N'-*((cyclohexane-1,4-diylbis(oxy))bis(2-oxoethane-2,1-diyl))bis(*N,N-*dimethylalkan-1-aminium) methyl sulfate[CHOGS-8, CHOGS-12 and CHOGS-16 compounds].* Synthesized compounds **III** (10 mmole) was added to a single-neck flask containing 43 mmol dimethylsulphate in tetrahydrofuran as a solvent for 72 h at room temperature. Semisolid and viscous materials were produced. The obtained products were washed several times with diethylether to remove the unreacted materials and to afford the required cationic gemini surfactants.

The prepared compounds were elucidated by The FT-IR spectrum (recorded in KBr on a thermo Nicolet iS10 FTIR spectrophotometer), ^{1}H NMR (400 MHz) and ^{13}C NMR (100 MHz) spectra (measured in DMSO-d_6 using FT-IR-ALPHA-BRUKER-Platinum-ATR).

2.2.2. Electrochemical measurements

Electrochemical experiments were performed in a traditional three-electrode consisted of: a saturated calomel electrode as reference (SCE), a platinum sheet as a counter electrode, and C1018 carbon steel as working electrode (WE). To obtain steady state open circuit potential (E_{ocp}) the carbon steel electrodes were immersed in the tested solution for 50 min before starting the measurements. Impedance measurements (EIS) were carried out at open circuit potential (E_{ocp}) with the AC voltage amplitude 10 mV in the frequency range from 100 kHz to 0.5 Hz. All of measurements were conducted with VersaSTAT4 potentiostat/Galvanostat connected to laptop. The potentiodynamic polarization curves were scanned from −250 mV vs. E_{ocp}, to +250 mV vs. E_{ocp} at a scan rate of 1.0 mV s^{-1}. All measurements were accomplished at 333 K. In order to obtain the impedance parameters, the experimental data was fitted to the equivalent circuit model using the fit and simulation tool of the Z-View software. All the measurements were carried out in triplicate and the corrosion parameters values recorded as mean ± standard deviation.

2.2.3. Weight loss measurements

The carbon steel specimens used for weight loss measurements have a rectangular form (3.5 cm × 2 cm × 0.5 cm). They were abraded with different grade of emery paper washed with distilled water, and dried in acetone and warm air. The specimens were weighed and then immersed for up to 24 h in a solution containing 15% HCl with and without different concentrations of each surfactant. Afterwards, the steel sheets were taken out, rinsed thoroughly with distilled water, dried, and accurately weighed.

2.2.4. Surface tension measurements

The surface tension of aqueous solutions was measured by Tensiometer-K6 processor (KRÜSS company, Germany) using the ring method and each sample were determined from the average of three times measurements. All the surfactants aqueous solutions were allowed to stand 3 h before measured, and all measurements were performed under 298 K. Before measurements, the surface tension of the doubled distilled water was confirmed in the range of 72.0 ± 0.3 mN/m.

2.2.5. Biodegradability

In the river water, the biodegradability test of the synthesized cationic gemini surfactants CHOGS-8, CHOGS-12 and CHOGS-16 was carried out using the surface tension method (Du Noüy Tensiometer (KRÜSS K6 tensiometer) at 25 °C [25]. In this method, each surfactant was dissolved in river water with a concentration of 100 ppm and incubated at 298 K. A sample was withdrawn daily

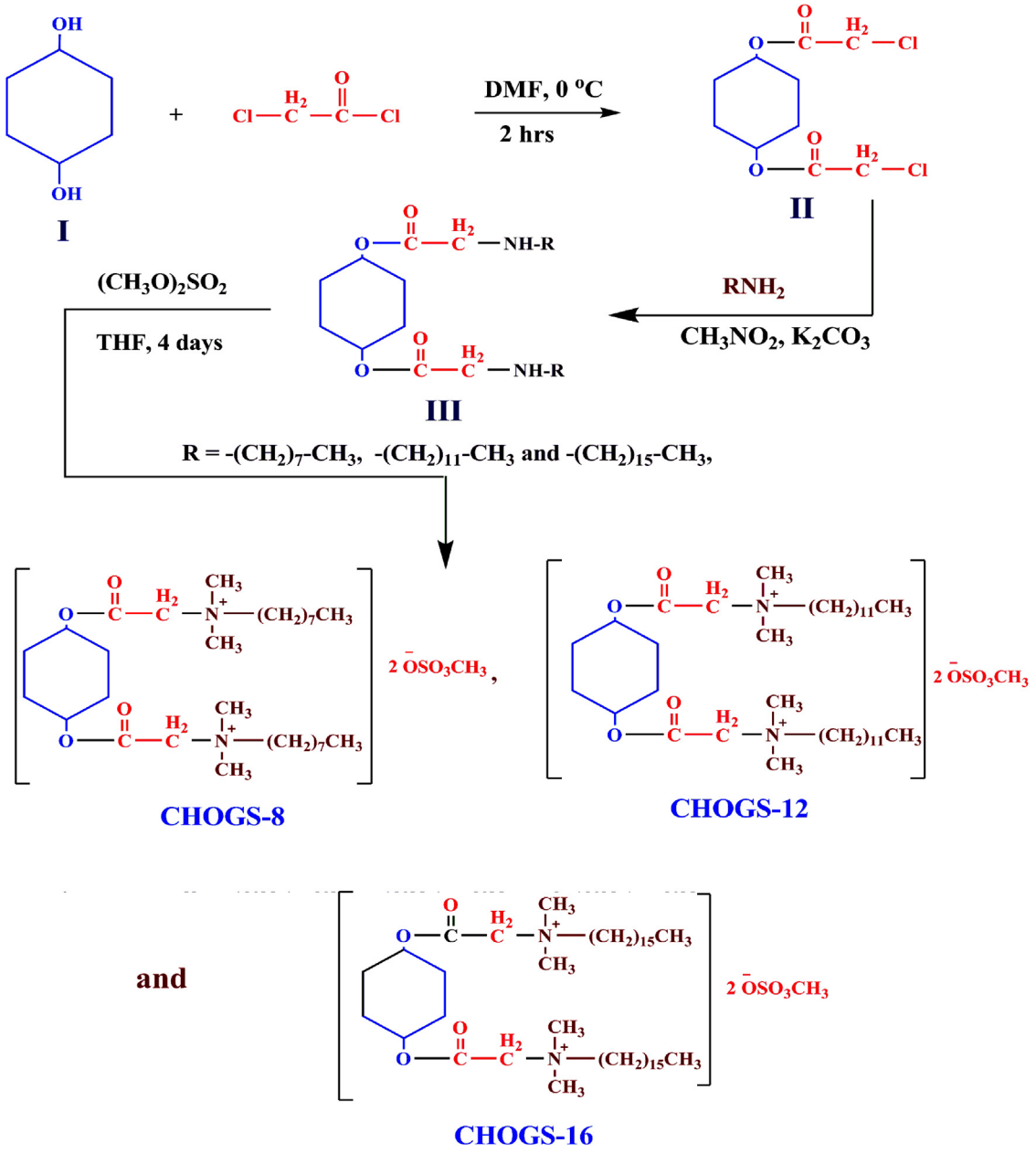

Fig. 1. General scheme for synthetic procedure of cyclohexane cationic gemini surfactants (CHOGS-8, CHOGS-12 and CHOGS-16).

(for 21 days), filtered and the surface tension value was measured three times and the recorded values were taken as the average. Surface tension measurements were made periodically (each day) on each sample during the degradation [26,27]. The biodegradation percent (D%) was calculated using Eq. (1):

$$D(\%) = \frac{\gamma_t - \gamma_0}{\gamma_{bt} - \gamma_0} \times 100 \quad (1)$$

where: the surface tension at time 0 is γ_0, the surface tension at time t is γ_t and γ_{bt} is the surface tension of river water without addition of surfactants at time *t*.

2.2.6. Electrical conductivity measurements

Electrical conductivity of surfactant solutions was performed on a conductivity meter (model Type AD3000; EC/TDS and Temperature meter) at 298 K. The measurement was repeated three times for each solution.

2.2.7. Surface characterization

For surface morphological investigations of the carbon steel samples in the acidic solutions with and without the optimal concentration of the inhibitors, scanning electron microscopic and energy dispersive X-ray spectroscopy analysis (SEM/EDX) were performed used the JOL JSM-5500 LV scanning electron microscope (JOL-Japan) equip with energy dispersive X-ray microanalyzer.

2.2.8. Computational approaches

Quantum chemical calculations were carried out using Gaussian 09 program package [28] at B3LYP/6–31 G (d, p) level of theory [29]. Some of electronic parameters such as energy of the highest occupied molecular orbital (E_{HOMO}), energy of the lowest unoccupied molecular orbital (E_{LUMO}), energy gap (ΔE), chemical hardness (η), softness (σ), ionization potential (I_p), electron affinity (E_A), electronegativity (χ), the fraction of electron transferred (ΔN) and dipole moment (μ) of the investigated cationic gemini surfactants were calculated.

3. Results and discussion

3.1. Structure confirmation of the synthesized cationic gemini surfactants (CHOGS)

The spectroscopic data obtained from analysis of the CHOGS compounds are as follows:

3.1.1. Cyclohexane-1,4-diyl bis(2-chloroacetate) [compound II]

White color, solid, mp = 145 °C, Yield = 95%. FT-IR (KBr pellet) shows characteristic bands at 2921, and 2869 cm^{-1} (νC—H aliphatic), 1749 cm^{-1} ($\nu_{C=O}$ of ester), and 1183 cm^{-1} (ν_{C-O-C}) (Fig. S1a; supporting data).

^{1}H NMR (400 MHz) δ (ppm) (DMSO-d_6):1.55-1.91 (q, 8H, 4 [**CH2**-]), 4.45 (s, 4H,2[Cl-**CH2**CO]), 4.81 (t, 2H, **[CH**-O]) (Fig. S1b; supporting data).

3.1.2. Cyclohexane-1,4-diyl bis(2-(alkylamino) acetate [compound III]

FT-IR (KBr pellet) displays distinctive bands at 3151 cm^{-1} (ν_{NH}), 2923, 2950 and 2852 cm^{-1} (ν_{C-H}, aliphatic fatty chain), 1736 cm^{-1} ($\nu_{C=O}$ of ester), and 1189 cm^{-1} (ν_{C-O-C}).

3.1.3. N,N′-((Cyclohexane-1,4-diylbis(oxy))bis(2-oxoethane-2,1-diyl))bis(N,N-dimethyloctan-1-aminium) methyl sulfate [CHOGS-8]

Yellow oily liquid, yield = 80%, FT-IR (KBr pellet) cm^{-1} = 2921, and 2869 (ν_{C-H}, aliphatic fatty chain), 1750 ($\nu_{C=O}$ of ester), and 1220 (ν_{C-O-C}) (Fig. S2a; supporting data).

^{1}H NMR (400 MHz) δ (ppm) (DMSO-d_6): 0.92 (t, 6H, 2**[CH3**-CH_2]), 1.3 (s, 20H,2[$(CH_3$-**CH2**-$)_5$]), 1.72 (m, 4H, 2**[CH2**-CH_2 -N^+]), 1.98-2.12 (m, 8H, 2[-CH-**CH2**-**CH2**CH]), 3.21 (t, 4H, 2**[CH2**-N^+]), 4.11(m, 12H, 2[**(CH3)2**-N^+]), 4.81(s, 4H, 2[CO-**CH2**-N^+]), 4.97(m, 2H, 2**[CH**-O]) (Fig. S2b; supporting data).

^{13}C NMR (100 MHz) δ (ppm) (DMSO-d_6): 14.11 [2(**CH3**-CH_2)], 22.25 [2(-**CH2**-CH_3)], 25.22 [2**(CH2**-CH_2 -N^+)], 27.81 [2(-CH-**CH2**-**CH2**CH)], 29.58 [2(CH_3CH_2-**CH2**$)_5$], 31.11 [2(**CH2**-CH_2CH_3)], 49.33 [2**(C O-CH2**-N^+)], 53.23 [2**((CH3)2**-N^+)], 58.31 [2**(CH2**-N^+)], 66.12 [2**(CH**-O)], 190.12 [**C**=O, carbonyl ester] (Fig. S2c; supporting data).

3.1.4. N,N′-((Cyclohexane-1,4-diylbis(oxy))bis(2-oxoethane-2,1-diyl))bis(N,N-dimethyldodecan-1-aminium) methyl sulfate [CHOGS-12]

Brown viscous liquid, yield = 85%, FT-IR (KBr pellet) cm^{-1} = 2920, and 2862 ((ν_{C-H}, aliphatic fatty chain), 1752 ($\nu_{C=O}$ of ester), and 1221 (ν_{C-O-C}) (Fig. S3a; supporting data).

^{1}H NMR (400 MHz) δ (ppm) (DMSO-d_6): 0.93 (t, 6H, 2 **[CH3**-CH_2]), 1.32 (s, 20H, 2 [CH_3-**CH2**$]_5$), 1.72 (m, 4H, 2 **[CH2**-CH_2 -N^+]), 3.03-3.19 (m, 8H, 2 [-CH-**CH2**-**CH2**CH]), 3.25 (t, 4H, 2 **[CH2**-N^+]), 3.4 (m, 12H, 2 [**(CH3)2**-N^+]), 3.71 (s, 4H, 2 **[C O-CH2**-N^+]), 3.9 (m, 2H, 2 **[CH**-O]) (Fig. S3b; supporting data).

^{13}C NMR (100 MHz) δ (ppm) (DMSO-d_6): 14.78 [2(**CH3**-CH_2)], 24.25 [2(-**CH2**-CH_3)], 27.22 [2**(CH2**-CH_2 -N^+)], 28.34 [2(-CH-**CH2**-**CH2**CH)], 31.58 [2(CH_3CH_2-**CH2**$)_8$], 33.11 [2(**CH2**-CH_2CH_3)], 49.83 [2**(C O-CH2**-N^+)], 52.55 [2**((CH3)2**-N^+)], 59.37[2**(CH2**-N^+)], 64.49 [2**(CH**-O)], 168.12 [**C**=O, carbonyl ester] (Fig. S3c; supporting data)

3.1.5. N,N′-((Cyclohexane-1,4-diylbis(oxy))bis(2-oxoethane-2,1-diyl))bis(N,N-dimethylhexadecan-1-aminium) methyl sulfate [CHOGS-16]

Yellowish-white semisolid, yield = 87%, FT-IR (KBr pellet) cm^{-1} = 2923, and 2861 (ν_{C-H}, aliphatic fatty chain), 1751 ($\nu_{C=O}$ of ester), and 1219 (ν_{C-O-C}).

^{1}H NMR (400 MHz) δ (ppm) (DMSO-d_6): 0.90 (t, 6H, 2 **[CH3**-CH_2]), 1.30 (s, 20H, 2 [CH_3-**CH2**$]_5$), 1.72 (m, 4H, 2 **[CH2**-CH_2 -N^+]),

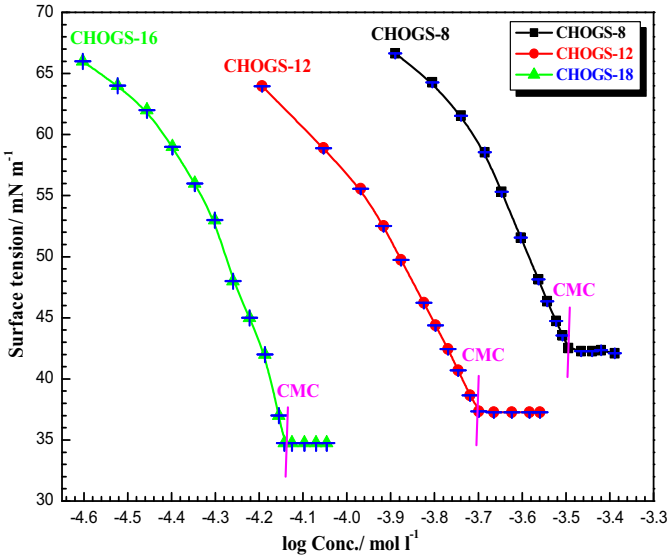

Fig. 2. Variation of the surface tension with the concentration of the synthesized cationic gemini surfactants in water at 25 °C.

3.03-3.19 (m, 8H, 2 [-CH-**CH2**-**CH**$_2$CH]), 3.25 (t, 4H, 2**[CH2**-N^+]), 3.4 (m, 12H, 2 [**(CH3)2**-N^+]), 3.71 (s, 4H, 2 **[C O-CH2**-N^+]), 3.82 (m, 2H, 2**[CH**-O]).

^{13}C NMR (100 MHz) δ (ppm) (DMSO-d_6): 14.66 [2(**CH3**-CH_2)], 25.07 [2(-**CH2**-CH_3)], 28.43 [2**(CH2**-CH_2 -N^+)], 29.89 [2(-CH-**CH2**-**CH2**CH)], 33.77 [2(CH_3CH_2-**CH2**$)_{12}$], 39.88 [2(**CH2**-CH_2CH_3)], 54.78 [2**(C O-CH2**-N^+)], 58.92 [2**((CH3)2**-N^+)], 65.76 [2**(CH2**-N^+)], 72.55 [2**(CH**-O)], 165.66 [**C**=O, carbonyl ester].

3.2. Surface activity and electrical conductivity measurements

The surface tension measurement (γ) of the aqueous solutions of gemini surfactants to the logarithm of concentration at 298 K had been drawn in Fig. 2. The plots of γ versus log C show a break point at a certain concentration corresponding to the CMC of the three gemini surfactants. From Fig. 2, the CMC value and the surface tension at the CMC (γ_{CMC}) are showed in Table 1. It can be noted that the synthesized gemini surfactant with longer hydrophobic chains has a lower CMC value. Also as the length of hydrophobic chain increases, the value of CMC decreased gradually for the enhanced hydrophobic interaction between the longer alkyl chains.

Besides, the CMC and degree of counter ion dissociation (α) calculated from the ratio of the slopes above and below the break indicative of the CMC as shown in Fig. 3. The degree of counter ion binding (β) could be obtained by using the following relationship: β=1-α. All values of α and β are listed in Table 1, it can be noted that the values of β increase slightly with increasing hydrophobic alkyl chain length at the appropriate temperature. Also the CMC values have been determined using electrical conductivity and agreed with those obtained from the surface tension.

From the values of surface tension (γ_{CMC}) at CMC, the effectiveness values (the maximum reduction of surface tension, π_{CMC}) were determined using the following expression:

$$\pi_{CMC} = \gamma_0 - \gamma_{CMC} \quad (2)$$

where the surface tension at CMC is γ_{CMC} and the surface tension measured for pure water is γ_0, the maximum reduction of surface tension can be used to evaluate the effectiveness of surfactant to lower the surface tension of water. From the data observed in Table 1, it can be seen that the values *of* π_{CMC} increased with increasing the hydrocarbon chain length. As well as the results showed that the synthesized compound CHOGS-16 more effective

Table 1
Surface active properties of the synthesized cationic gemini surfactant compounds (CHOGS-8, CHOGS-12 and CHOGS-16).

Compounds	CMC[a]/mM	CMC[b]/mM	γ_{CMC}/mN m^{-1}	π_{CMC}/mN m^{-1}	α	β	Γ_{max}/mol cm^{-2}	A_{min}/nm^2	ΔG^0_{mic}/kJ mol^{-1}	ΔG^0_{ads}/kJ mol^{-1}
CHOGS-8	0.320	0.267	42.52	29.48	0.54	0.46	3.30×10^{10}	0.50	−29.08	−29.96
CHOGS-12	0.200	0.216	38.34	33.66	0.43	0.57	3.80×10^{10}	0.43	−33.13	−33.99
CHOGS-16	0.072	0.067	34.78	37.22	0.40	0.60	4.03×10^{10}	0.41	−37.81	−38.72

[a] CMC values obtained from surface tension measurements.
[b] CMC values obtained from conductivity measurements.

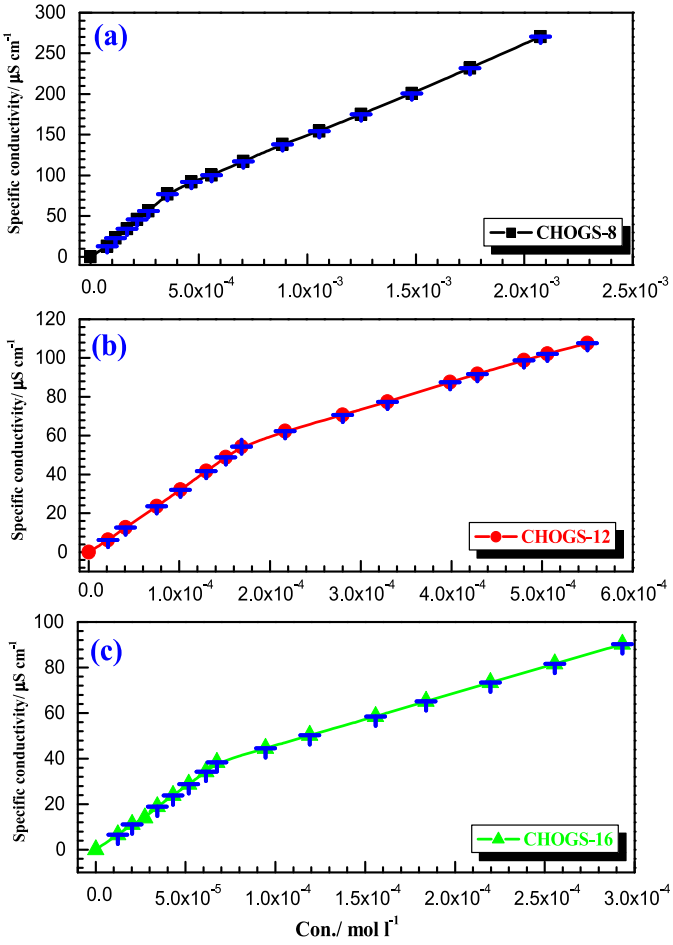

Fig. 3. Plotting of specific conductivity against concentration of the synthesized cationic gemini surfactants (a) CHOGS-8, (b) CHOGS-12 and (c) CHOGS-16 in water at 25 °C.

surfactant, which realized the maximum reduction of the surface tension at CMC reach to 37.22 mN m^{-1} [30]. At the air-water interface, the packing densities of the synthesized three gemini surfactants are very important to interpret the surface activities of different gemini surfactants. The calculation of maximum surface excess concentration at the air/water interface (Γ_{max}) can be carried out via Gibb's isotherm equation (3) [31]:

$$\Gamma_{max} = \frac{-1}{2.303nRT}\left(\frac{d\gamma}{d\log C}\right)_T \quad (3)$$

where R is a gas constant; $d\gamma$/dlogC is the slop of γ vs log C; T is the absolute temperature; and n is the number of ions dissociation that originate in solution by presence the surfactant. The value of n is taken to be 3 for synthesized gemini surfactants which are a divalent surfactant ion and two univalent counter ions [32,33]. The

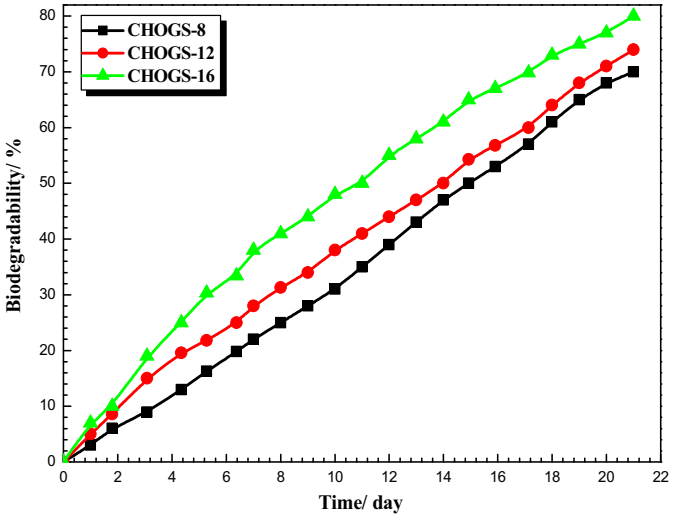

Fig. 4. Variation of biodegradation (%) with (day) the time for the synthesized cationic surfactants.

minimum area occupied per surfactant molecule at the air/water interface (A_{min}) is calculated via Eq. (4) [34]:

$$A_{min} = \frac{10^4}{\Gamma_{max} \times N_A} \quad (4)$$

where N_A is Avogadro's number, A_{min} is in nm^2. From Table 1, it is found that the values of Γ_{max} increased but A_{min} decreased by increasing the length of hydrophobic chain, the interactions of hydrophobic are developed with the increase of hydrocarbon chain length, which make the gemini cyclohexane surfactant molecules pack more closely, then the Γ_{max} values increase [34–36]. Also it showed that the gemini cyclohexane surfactants with two hydrocarbon chain length could pack more closely than the conventional surfactants at the air/water interface.

The standard Gibbs free energy change of micellization (ΔG^0_{mic}) and adsorption (ΔG^0_{ads}) of synthesized cationic gemini surfactants were calculated according the following equations [37]:

$$\Delta G^0_{mic} = (2-\alpha)RT \ln CMC \quad (5)$$

$$\Delta G^0_{ads} = (2-\alpha)RT \ln CMC\text{-}0 \times 06\pi_{CMC}A_{min} \quad (6)$$

where CMC is the critical micelle concentration, R is a gas constant, T is the absolute temperature, π_{CMC} is the effectiveness; α is a degree of counter ion dissociation and A_{min} is the minimum area occupied per surfactant molecule at the air/water interface. From the data listed in Table 1, it can be concluded that the values of ΔG^0_{ads} are all negative and greater than those of ΔG^0_{mic}. These observations are consistent with the data reported previously [37], which indicated that the surfactant molecules prefer to be adsorbed on the metal surface rather than form micelles [34].

Table 2
Electrochemical parameters and inhibition efficiency obtained from polarization measurements for carbon steel in 15% HCl in the absence and presence of various concentrations of gemini surfactant inhibitors at 60 °C.

Inhibitors code	C_{inh}/ppm by weight	C_{inh}/mM	i_{corr}/mAcm^{-2}	-E_{corr}/mV (SCE)	β_a/mV dec^{-1}	-β_c/mV dec^{-1}	θ	P_{PDP}/%
Blank	**0.0**	**0.0**	**2.431 ± 0.0780**	**452**	**122**	**223**	–	–
CHOGS-8	25	0.04882	0.84040 ± 0.031	472	129	219	0.654	65.43
	50	0.09764	0.68506 ± 0.026	468	129	234	0.718	71.82
	100	0.19528	0.35225 ± 0.018	466	126	237	0.855	85.51
	150	0.29292	0.17892 ± 0.014	472	127	210	0.926	92.64
	200	0.39056	0.07512 ± 0.011	471	132	228	0.969	96.91
CHOGS-12	25	0.040	0.73562 ± 0.017	470	129	236	0.697	69.74
	50	0.080	0.52850 ± 0.012	471	134	229	0.782	78.26
	100	0.15999	0.23775 ± 0.015	468	129	222	0.902	90.22
	150	0.23999	0.10940 ± 0.012	459	129	224	0.955	95.50
	200	0.31998	0.04303 ± 0.013	455	133	228	0.982	98.23
CHOGS-16	25	0.03391	0.64592 ± 0.015	470	127	238	0.734	73.43
	50	0.06782	0.41230 ± 0.019	467	130	218	0.830	83.04
	100	0.13564	0.16725 ± 0.014	466	129	229	0.931	93.12
	150	0.20346	0.06928 ± 0.015	467	128	231	0.971	97.15
	200	0.27128	0.01920 ± 0.0017	465	129	236	0.992	99.21

3.3. Biodegradability

Using the Die-Away test, the biodegradability of the synthesized cationic gemini surfactants was evaluated for 21 day and presented in Fig. 4. The biodegradation results in the river water reflected the fact that, lowering of the surface tension value is a reverse function of biodegradation. From the data in Fig. 4, it is noted that the biodegradation ratios of the gemini surfactants ranged between 70 and 80% after 21 day. Also it is found that the biodegradation extent of different gemini surfactant solutions increase gradually by increasing the time and reached a maximum values after 21 days. In addition, there is a direct relationship between the length of hydrophobic chain and the rate of biodegradation. From Fig. 4, the biodegradation increased with increased linearity of the hydrophobic chain length group (fatty chain) and decreased as the number of hydrophobic chain groups increased. These results agreed to the in Ref. [38]. As well as the results showed that the biodegradability of CHOGS-16 > CHOGS-12 > CHOGS-8, and the biodegradation values of these cationic gemini surfactants are lower than conventional cationic surfactants [39]. Consequently, these compounds can be classified as biodegradable surfactants in the open environment. In fact, the biodegradation affinity is due to the presence of an oxycarbonyl group (—O—C=O—) which has the ability to degrade by the action of the environmental microorganisms.

3.4. Weight loss measurements

The values of corrosion rate and inhibition efficiency (P_W%) were obtained from weight loss measurements in the absence and presence of different concentrations of the investigated cationic gemini surfactants at 333 K are presented in Fig. 5. It was found that, the corrosion rate value in 15% HCl without inhibitors is 3.6269 ± 0.21 mg cm^{-2} h^{-1} and decreased to 0.09031 ± 0.0062, 0.04606 ± 0.0034 and 0.01414 ± 0.0011 mg cm^{-2} h^{-1} in the presence of 200 ppm of CHOGS-8, CHOGS-12 and CHOGS-16, respectively. Furthermore, at a constant concentration of the surfactant, the corrosion rate is decreased by increasing the hydrophobic chain length of the surfactants, which favors their adsorption at the metal/acid interface. The inhibition efficiency of all surfactants was increased with increasing the concentration. The maximum inhibition efficiency for each compound was obtained at 200 ppm. The inhibition of the corrosion processes by the CHOGS surfactants in acidic media revealed the adsorption of these inhibitors at the metal surface [25].

3.5. Potentiodynamic polarization measurements

The use of potentiodynamic polarization measurements can be provided important information about the kinetics of corrosion reactions [40]. The potentiodynamic polarization plots of carbon steel in 15% HCl solution containing different concentrations of CHOGS-8, CHOGS-12 and CHOGS-16 at 60 °C are presented in Fig. 6(a), (b) and (c), respectively. Given in Fig. 6, in the presence of investigated inhibitors both cathodic and anodic Tafel curves shift towards minimize the current densities. This decrease is more pronounced with increasing of the inhibitor concentration. This observation demonstrates that the inhibitors are adsorbed on the carbon steel surface [7]. The electrochemical corrosion kinetic parameters, such as cathodic and anodic Tafel slopes (β_c and β_a), corrosion current density (i_{corr}) and the corrosion potential (E_{corr}) obtained by extrapolating the cathodic and anodic Tafel curves to the point of intersection [3], are listed in Table 2. The corrosion inhibition efficiency (P_{PDP}%) and surface coverage (θ) from the polarization measurements were estimated from the obtained i_{corr} values using the following relationship [41]:

$$P_{PDP}/\% = \left(1 - \frac{i_{corr(i)}}{i_{corr(0)}}\right) \times 100 = \theta \times 100 \quad (7)$$

where $i_{corr(i)}$ and $i_{corr(0)}$ are the inhibited and uninhibited corrosion current densities, respectively. As observed from the polarization graph (Fig. 6), the presence of CHOGS inhibitors in HCl solution resulted in a slight shift of E_{corr} toward the negative direction in comparison with the inhibitor free solution. These findings indicate that both the anodic dissolution of metal and cathodic hydrogen evolution reactions were inhibited after the addition of investigated surfactants to the aggressive medium. Therefore, these compounds could be classified as mixed-type inhibitors with predominant control of cathodic reaction [42–44].

Based on the data in Table 2, the i_{corr} decreased gradually with increasing the inhibitor concentration, indicating that the inhibitor has an effective inhibition for the carbon steel corrosion. Furthermore, the introducing of the surfactant molecule did not cause significant displacement in the β_c and β_a values. This indicates that the carbon steel corrosion mechanism in HCl solution does not alter after addition the studied surfactants. Namely, the corrosion inhibition is caused by blocking the available reaction sites on the surface of steel without modifying the corrosion mechanism in the titled aggressive media. The surface coverage (θ) increases with increase in concentration of inhibitor. From Table 2, it is clearly observed that

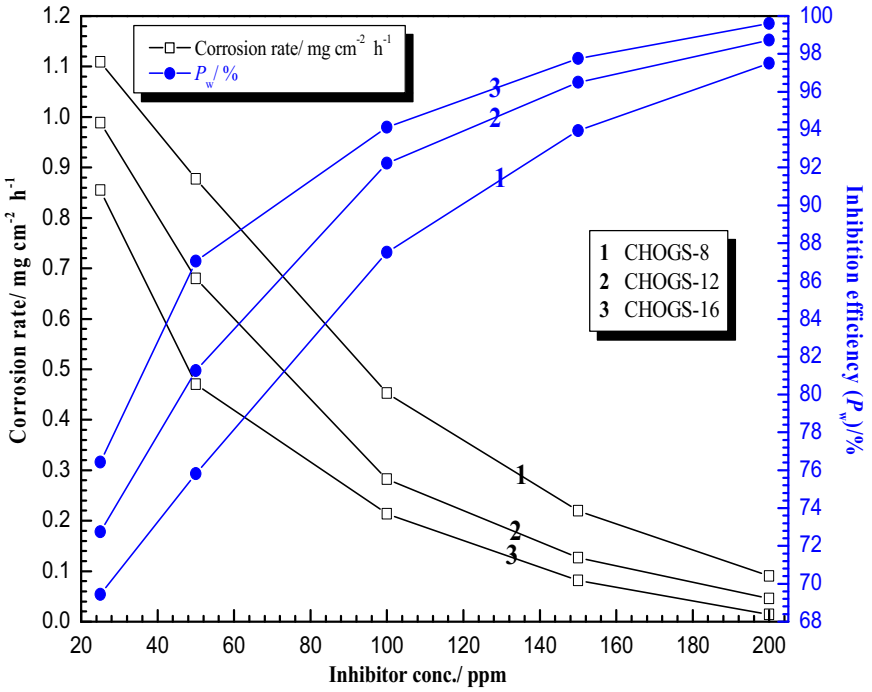

Fig. 5. Variation of the corrosion rate and inhibition efficiency with the concentration of the studied inhibitors in ppm for carbon steel in 15% HCl at 333 K.

the inhibition efficiency increase with the increase in the inhibitor concentrations applied in the study. It is logical to deduce that the protection performance could be caused by the formation of the adsorption film resulting from the interaction between quaternary nitrogen atom (N^+) and carbon steel surface.

When we compared our study with the literature data, e.g. Hegazy et al. [45] measured the behaviors of inhibition of some cationic gemini surfactants namely: bis(p-(*N*,*N*,*N*-octyldimethylammonium bromide) benzylidene) benzene-1,4-diamine (I), bis (p-(*N*,*N*,*N*-decyldimethyl-ammonium bromide)-benzylidene) benzene-1, 4-diamine (II), and bis(p-(*N*,*N*,*N*-dodecyldimethylammonium bromide) benzyli-dene) benzene-1,4-diamine (III) on carbon steel in 1.0 M HCl. The inhibition efficiencies increased with the increase in inhibitor concentration and ranged between 93.3% and 93.77%, respectively. Wang et al. [41] also investigated the inhibition performance of a cationic gemini-surfactant (1,4-bis (1-chlorobenzyl-benzimidazolyl)-butane) on mild steel in 0.25 M H_2SO_4 solution. The results showed that, the inhibition efficiency of this inhibitor was 97% in the presence of 37 μM. As another study, Hegazy et al. [46] studied the inhibition effect of cationic gemini surfactant namely, 2, 2′-(pentane-1,5-diylidenebis(azan-1-yl-1-ylidene)) bis (1-1 dodecylpyridinium bromide) on carbon steel in 0.5 M H_2SO_4. They found that, in the presence of 0.01 M of compound the inhibition efficiency was around 94.9%. As for the investigated cationic gemini surfactants, P_{PDP}% values increased as a function of the concentration of inhibitor, and exhibited the highest value at 200 ppm of cationic gemini surfactant. The inhibition efficiencies of the three investigated compounds by potentiodynamic polarization measurements decreased in the following order: CHOGS-16 (99.21%) > CHOGS-12 (98.23) > CHOGS-8 (96.91%).

3.6. Electrochemical impedance spectroscopy measurements (EIS)

To further confirm the protection ability of the synthesized gemini surfactants, EIS measurements were performed in 15% HCl solution at 60 °C. The Nyquist plots of carbon steel corrosion in acidic solutions in the absence and presence of various concentrations (25-200 ppm) of the surfactants CHOGS-8, CHOGS-12 and CHOGS-16 are presented in Fig. 7a, b and c, respectively. The Nyquist plots of the carbon steel electrode immersed in different concentrations of the investigated inhibitors all have depressed single semicircles (one time constant) with a center under the real axis at high frequency range. This event can be attributed to the change on the morphology of the electrode surface resulting from surface roughness and other inhomogeneities of the electrode [47,48]. It is obvious from Fig. 7 the diameter of semicircle significantly increases when CHOGS-8, CHOGS-12 and CHOGS-16 inhibitors are introducing into the corrosive media, indicating that the titled surfactants can inhibit the carbon steel corrosion in 15% HCl solution. The larger diameter of semicircle measured in the presence of CHOGS-16 compound reveals the inhibition effect of CHOGS-16 is better than that of CHOGS-8 and CHOGS-12 compounds. Furthermore, the capacitive loops diameters increase sharply with increment of CHOGS inhibitors dose and the shape of the loops does not alter.

Fig. 8a, b, c, shows the Bode and phase plots for carbon steel corrosion immersed in 15% HCl solution containing various concentrations of the three surfactant inhibitors used at 60 °C. It is observed that only one phase peak at the middle frequency range; supported that there is only one time constant. Meanwhile, the increasing dose of CHOGS inhibitors leads to the increase in the impedance modulus at low frequency and the phase angle shifted to more negative values of at intermediate frequency, demonstrating the formation of a protective layer on the metal surface [49].

Based on the above results, The EIS data are analyzed through the Randle's equivalent circuit (Fig. 9) that includes the solution resistance (R_s), charge transfer resistance (R_{ct}) in a parallel combination with constant phase element (CPE). Similar circuit has been proposed by Hegazy et al. for the acidic corrosion inhibition of steel [46]. In order to obtain a more accurate and representative fit, the double layer capacitance (C_{dl}) was replaced by the constant phase

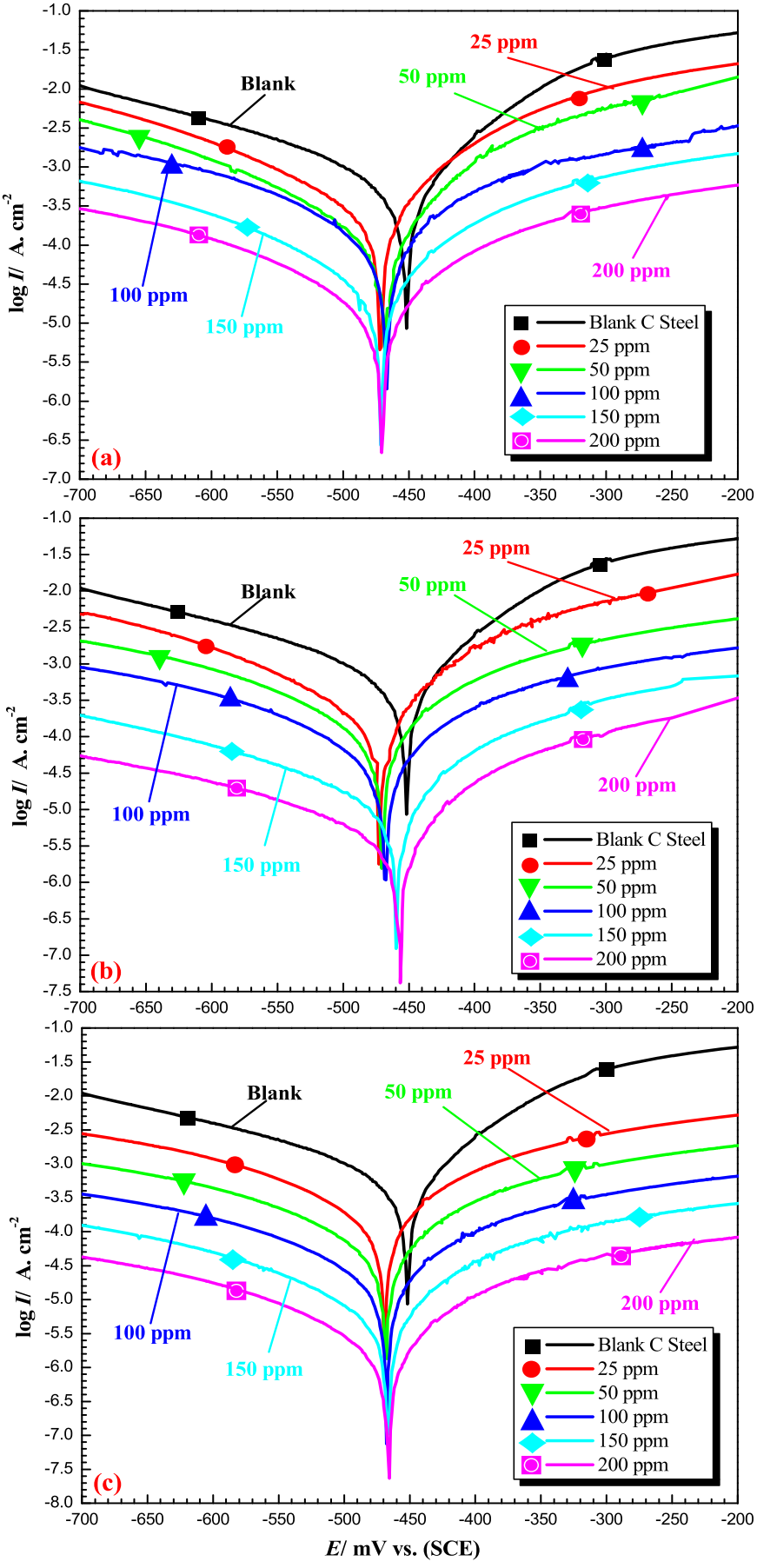

Fig. 6. Polarization curves of carbon steel in 15% HCl solution with or without different concentration of (a) CHOGS-8, (b) CHOGS-12 and (c) CHOGS-16 at 60 °C.

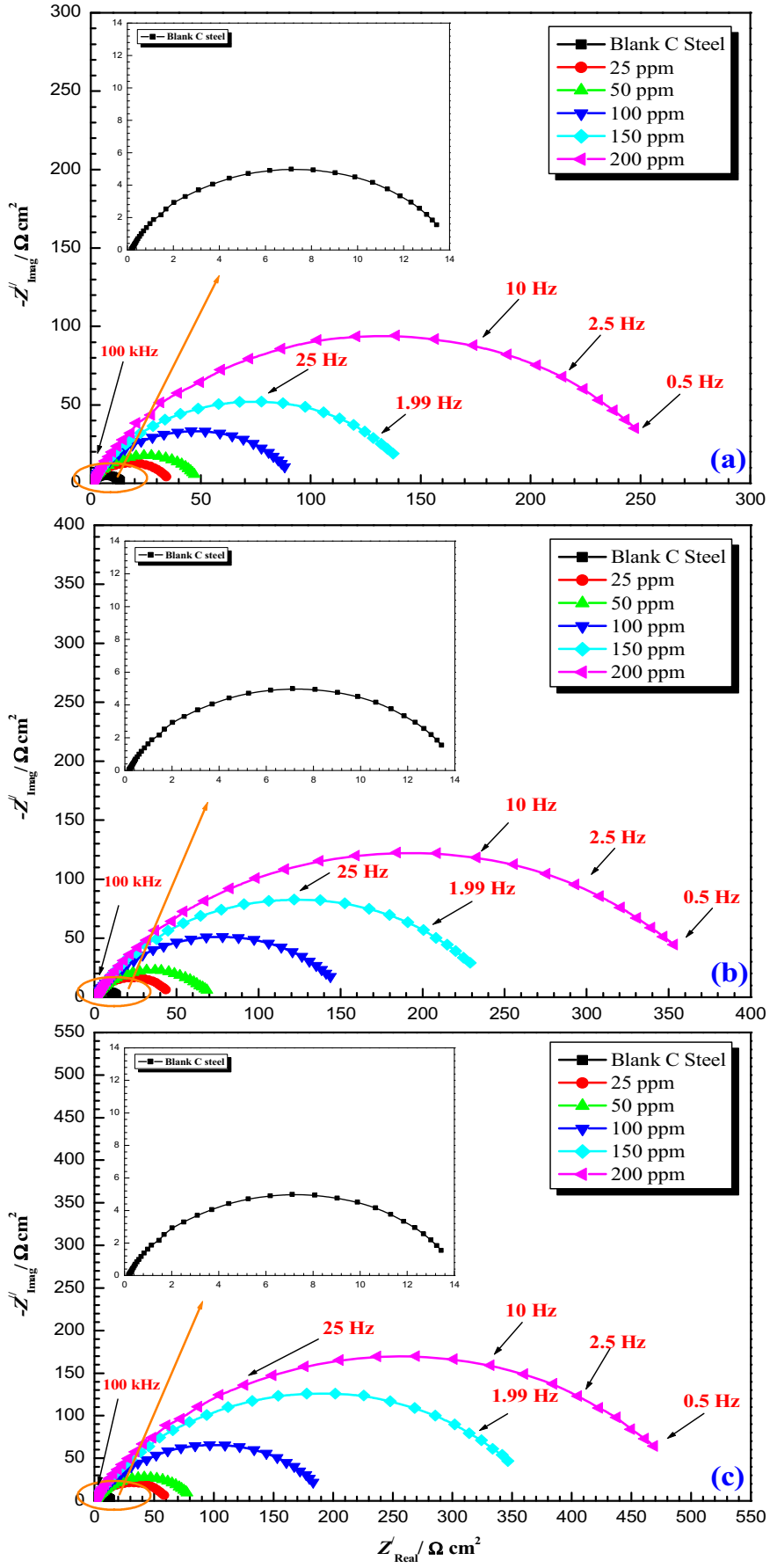

Fig. 7. Nyquist plots for carbon steel in 15% HCl in the absence and presence of various concentrations of the synthesized gemini surfactants (a) CHOGS-8, (b) CHOGS-12 and (b) CHOGS-16 at 60 °C.

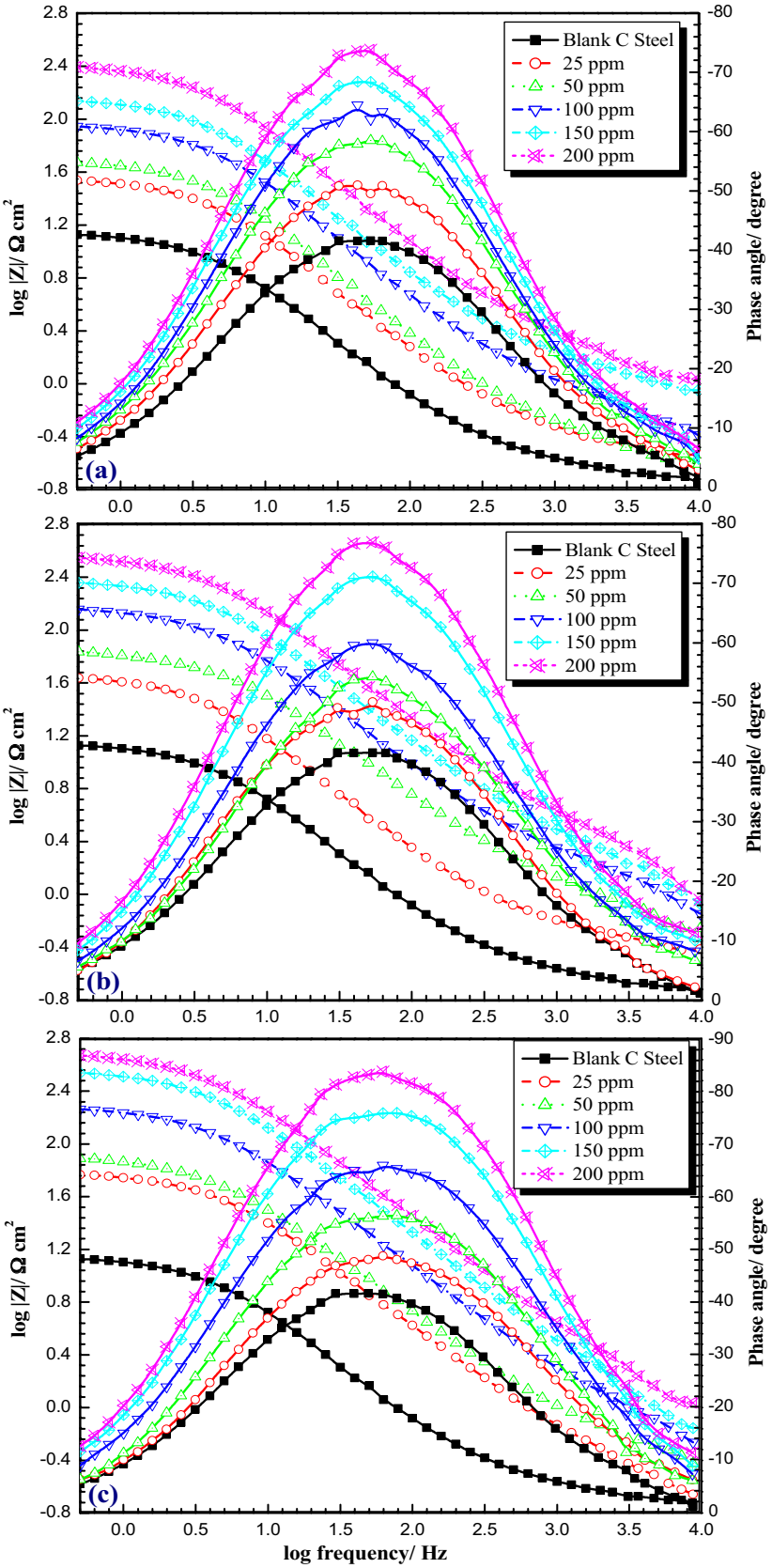

Fig. 8. Bode and Phase angle plots for carbon steel in 15% HCl in the absence and presence of various concentrations of the synthesized gemini surfactants (a) CHOGS-8, (b) CHOGS-12 and (b) CHOGS-16 at 60 °C.

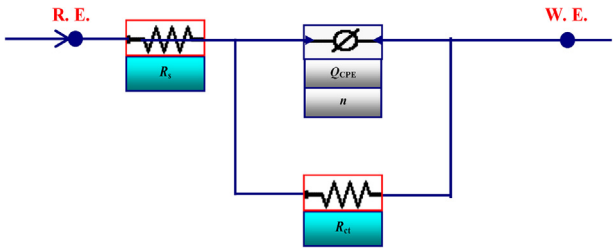

Fig. 9. Equivalent circuit used to fit the impedance spectra obtained for carbon steel/HCl interface in the absence and presence of CHOGS-8, CHOGS-12 and CHOGS-16 inhibitors.

element (CPE) as represented in Fig. 9. The CPE is given by the following expression [50,51]:

$$Q_{CPE} = Y_0^{-1}(j\omega)^{-n} \quad (8)$$

where $j = (-1)^{1/2}$ is the imaginary number, Y_0 stand for the CPE constant, ω is the angular frequency in rad s^{-1} ($\omega = 2\pi f$), where f is the frequency in Hz and n is the phase shift (exponent) which is regarding to the surface inhomogeneity degree [52]. Based on the value of n, CPE can represent resistance ($n = 0$, $Y_0 = R$), capacitance ($n = 1$, $Y_0 = C$), inductance ($n = -1$, $Y_0 = L$) or Warburg impedance ($n = 0.5$, $Y_0 = W$). The lower value of n (Table 3) for carbon steel in 15% HCl solution indicated surface inhomogeneity resulted from metal surface roughening due to corrosion. Introducing of the investigated surfactants n values were increased, suggesting reduction inhomogeneity of surface due to the adsorption of surfactant molecules. The double layer capacitances, C_{dl}, for a circuit including a CPE were calculated by the expression [53,54]:

$$C_{dl} = Y_0(\omega_m)^{n-1} \quad (9)$$

where $\omega_m = 2\pi f_{max}$, represents the angular frequency at the maximum value of the imaginary part. The fitted impedance parameters (R_{ct}, C_{dl}, n and Y_0) for the corrosion of carbon steel in 15% HCl solution containing different concentration of the synthesized gemini surfactants are listed in Table 3. The surface converge (θ) and the inhibition efficiency (P_{EIS} %) calculated from the R_{ct} values by the following equation [55,56]:

$$P_{EIS}/\% = \frac{R^i - R^0}{R^i} \times 100 = \theta \times 100 \quad (10)$$

where R^i and R° are corrosion resistances in the presence and absence of the inhibitors, respectively. According to Table 3, the value of R_{ct} increases with addendum of surfactant compounds as compared to the blank solution, while the value of C_{dl} decreases. The larger R_{ct} and the smaller C_{dl} are attributed to the formation of a protective layer at the steel/HCl interface, resulting in an increase in inhibition efficiency. The maximum P_{EIS}% reaches up to 94.41%, 96.15% and 97.19% in the presence 200 ppm of CHOGS-8, CHOGS-12 and CHOGS-16, respectively. Based on Helmholtz model [40]:

$$C_{dl} = \frac{\varepsilon^0 \varepsilon A}{d} \quad (11)$$

where ε°, ε, A and d are the free space permittivity, the local dielectric constant, the electrode area and thickness of the interfacial layer, respectively. The decrease in C_{dl} is due to increase in the thickness of electrical double layer. The further mention that the investigated gemini surfactants function by adsorption at the metal/acid solution interface leading to the formation of a protective layer. It is worth noting that the inhibition efficiencies obtained from the EIS measurements is consistent with that obtained from potentiodynamic polarization and weight loss measurements.

3.7. Adsorption behavior of CHOGS surfactant inhibitors

As known that, the adsorption isotherm can supply basic knowledge about the corrosion inhibition performance between carbon steel surface and CHOGS surfactant molecules. In order to describe the adsorption of CHOGS, different isotherms were applied to fit the experimental results, including Temkin, Flory–Huggins, Langmuir, Freundlich and Frumkin adsorption isotherms. The surface coverage values (θ) for the various concentrations of the investigated CHOGS surfactants have been utilized to illustrate the best adsorption isotherm to determine the adsorption process. According to the θ values obtained from potentiodynamic polarization data, it can be concluded that the best description of the adsorption behavior of CHOGS surfactants can be demonstrated by adsorption isotherm of Langmuir [57]:

$$\frac{C_{inh}}{\theta} = C_{inh} + \frac{1}{K_{ads}} \quad (12)$$

where, C_{inh} and K_{ads} are the inhibitor concentration and the equilibrium constant for adsorption- desorption process, respectively. The plots in Fig. 10 (C_{inh}/θ vs. C_{inh}) were found to be linear with a correlation coefficient (R^2) and slope values as given in Fig. 10 at 60 °C. The correlation coefficient (0.9987, 0.9996 and 0.9999 for CHOGS-8, CHOGS-12 and CHOGS-16, respectively) and slope values (0.947, 0.950 and 0.952 for CHOGS-8, CHOGS-12 and CHOGS-16, respectively) are near to unity indicating that the adsorption of these surfactants obey the Langmuir adsorption isotherm. The average

Table 3
Electrochemical impedance parameters for carbon steel in 15% HCl without and with various concentrations of the synthesized gemini surfactants at 60 °C.

Inhibitors code	C_{inh}/ppm by weight	C_{inh}/mM	$R_s/\Omega\,cm^2$	$R_{ct}/\Omega\,cm^2$	$C_{dl}/\mu F\,cm^{-2}$	Q_{CPE}		θ	P_{EIS}/%
						$Y_0/\mu.\Omega^{-1}\,s^n\,cm^{-2}$	n		
Blank	**0.0**	**0.0**	**0.2 ± 0.02**	**15.4 ± 1.2**	**103.39**	**1.67**	**0.78**	–	–
CHOGS-8	25	0.04882	0.50 ± 0.04	37.5 ± 2.4	42.45	0.69	0.88	0.589	58.94
	50	0.09764	0.64 ± 0.03	52.3 ± 3.5	30.44	0.42	0.89	0.705	70.55
	100	0.19528	0.93 ± 0.05	96.1 ± 4.6	16.56	0.29	0.90	0.839	83.97
	150	0.29292	1.40 ± 0.06	152.5 ± 6.4	10.44	0.15	0.91	0.899	89.91
	200	0.39056	1.59 ± 0.06	275.6 ± 7.2	5.77	0.08	0.92	0.944	94.41
CHOGS-12	25	0.040	0.42 ± 0.02	50.1 ± 2.9	31.78	0.53	0.89	0.692	69.26
	50	0.080	0.56 ± 0.04	75.2 ± 3.7	21.17	0.32	0.88	0.795	79.52
	100	0.15999	1.18 ± 0.06	159.3 ± 5.1	9.99	0.22	0.90	0.903	90.33
	150	0.23999	1.62 ± 0.09	256.5 ± 4.7	6.21	0.11	0.91	0.939	93.99
	200	0.31998	2.21 ± 0.15	400.9 ± 8.9	3.97	0.06	0.93	0.961	96.15
CHOGS-16	25	0.03391	0.38 ± 0.03	64.8 ± 2.4	24.57	0.41	0.91	0.762	76.23
	50	0.06782	1.10 ± 0.10	85.1 ± 4.5	18.71	0.25	0.92	0.819	81.91
	100	0.13564	1.31 ± 0.15	200.2 ± 6.8	7.95	0.17	0.91	0.923	92.31
	150	0.20346	2.33 ± 0.21	379.7 ± 6.7	4.19	0.09	0.95	0.959	95.94
	200	0.27128	3.12 ± 0.32	549.3 ± 9.3	2.89	0.05	0.97	0.971	97.19

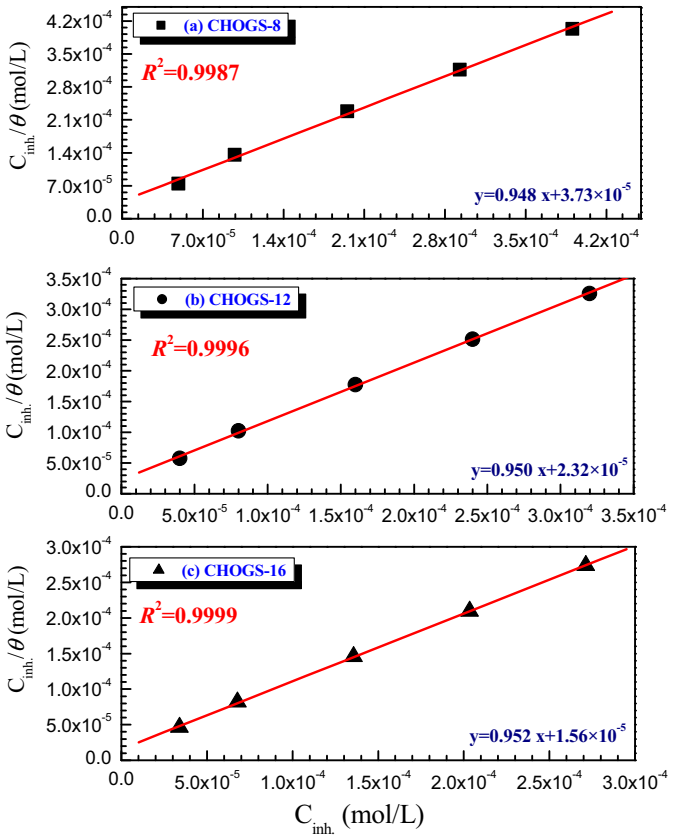

Fig. 10. Langmuir adsorption plots for carbon steel in 15% HCl solution at 333 K in various concentrations of (a) CHOGS-8, (b) CHOGS-12 and (c) CHOGS-16.

values of K_{ads} were calculated (from the intercept of Fig. 10) as 2.67×10^4, 4.30×10^4 and 6.41×10^4 M^{-1} for CHOGS-8, CHOGS-12 and CHOGS-16, respectively. The values of K_{ads}, are also related to the standard free energy of adsorption (ΔG^o_{ads}) based on the following equation [58]:

$$K_{ads} = \frac{1}{55.5} \exp\left(-\frac{\Delta G^0_{ads}}{RT}\right) \quad (13)$$

where R is the universal gas constant, T is the absolute temperature and the value of 55.5 is the molar concentration of water in the solution expressed in molarity unit [58]. The average values of ΔG^o_{ads} were found as −39.34, −40.65 and −41.76 kJ mol^{-1} for CHOGS-8, CHOGS-12 and CHOGS-16, respectively, indicated that the adsorption of these surfactants on carbon steel surface is a combination of both chemisorption and physisorption [59].

3.8. Surface characterization

EDX spectra and corresponding SEM micrographs of carbon steel specimens after immersed in 15% HCl in the absence and presence 200 ppm of CHOGS-8 and CHOGS-16 are presented in Fig. 11. Fig. 11a shows an SEM micrograph of the carbon steel specimen immersed in 15% HCl without inhibitors; it can be seen, the surface is very rough and badly damaged due to metal dissolution in hydrochloric acid solution. However, the presence of 200 ppm of CHOGS-8 and CHOGS-16 reduces the corrosion rate and surface damage has been diminished considerably (Figs. 11c, e) as compared to that in the absence of studied inhibitors (Fig. 11a), suggesting formation of a protective inhibitor film at the surface of carbon steel and also confirms the highest inhibition efficiency of the prepared gemini surfactants.

The results of EDX spectra are shown in Fig. 11(b, d and f). The EDX spectrum of carbon steel corrosion in blank HCl solution (Fig. 11b) described the characteristic signals of Fe, Mn, Si and K in addition to Cl and O elements, which shows that the oxide film covered specimen surface. However, the inhibited carbon steel (Fig. 11d, f) contains the peaks corresponding to Fe, Mn, K, O and Cl in addition to the elements present in the surfactant molecules (N and S elements), indicating the adsorption of inhibitor molecules at the metal surface.

3.9. Corrosion inhibition mechanism by the synthesized cationic gemini surfactants

The corrosion inhibition mechanism of steel in acidic environments by various organic compounds can be discussed based on molecular adsorption. The inhibitors were retarded the corrosion processes by formation of a physical barrier, changes in the electrical double layer and blocking both cathodic and anodic reactions. The investigated gemini surfactants molecules may be adsorbed at the steel surface by different types of adsorptions including electrostatic attraction between the charged metal and the charged molecules, interaction of unshared electron pairs in the studied molecule with the metal, and a combination of the above, i.e., surfactant can assignment by chemisorption, physisorption, or by complexation with the steel [60,61].

The prepared inhibitors adsorbed to the steel surface through the counter ion ($-SO_3^-$) on the anodic sites to reduce the anodic dissolution and quaternary nitrogen atom (N^+) on the cathodic sites to minimize the hydrogen evolution, i.e., physical adsorption. The high protection of the three synthesized surfactants was attributed to the occurrence of numerous adsorption centers (two quaternary nitrogen atoms and two ($-SO_3^-$ ions) and larger molecular size. The adsorption of gemini surfactants on electrode surface is more complicated than that of traditional surfactants because the gemini surfactants contain two hydrophobic groups and two hydrophilic groups. The adsorption of investigated gemini inhibitors on carbon steel surface was found to be obeyed Langmuir adsorption isotherm. The adsorptions of gemini surfactants on the steel surface in acidic solution take place through three various adsorption modes:

(i) At low concentrations, it obvious that the adsorption occurs through horizontal binding to hydrophobic region (Fig. 12a). This adsorption is preferable by an electrostatic interaction between the two ammonium groups (N^+) and cathodic sites on one hand and $-SO_3^-$ ions on the metallic surface on the other hand.

(ii) When the inhibitor concentration increases, a vertical adsorption takes place as a result of an inter-hydrophobic chain interaction (Fig. 12b).

(ii) At higher inhibition concentrations, a columnar adsorption of surfactant continues with the hydrophilic group popeyed into the solution and the hydrocarbon tail mingling with the adsorbed monomers, driven by the hydrophobic force, until the formation of a very rigid barrier of surfactant molecules on the steel surface (Fig. 12c).

The order of inhibition is decreased as the following order: CHOGS-16 (99.21%) > CHOGS-12 (98.23) > CHOGS-8 (96.91%). The higher P% values are attributed to their larger molecular size and the presence of two hydrophobic groups and two hydrophilic groups in the molecular structure of compounds. By a comparison of the inhibition efficiency (P%) between the studied compounds, the CHOGS-16 inhibitor displays higher P% values, which can be due to an increase in the length of hydrophobic chain. By increasing the geometric length, the isolation between metal-solution interactions increased and hence the efficiency of the corrosion increased. The chain length changes film properties such as surface tension, aggregate lifetime and etc. [62]. In our investigation, we studied

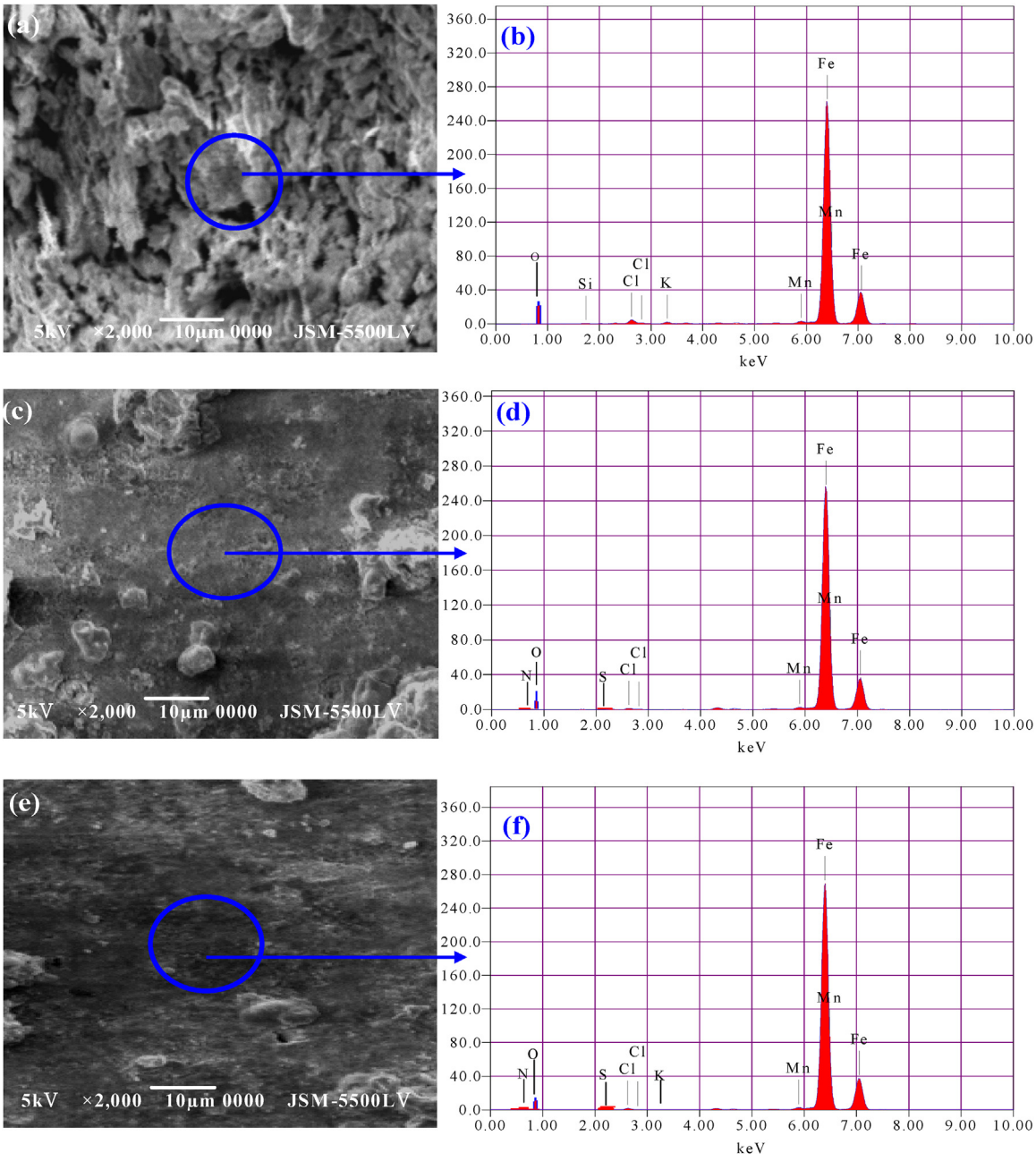

Fig. 11. SEM micrograph (a) and EDX analysis (b) of carbon steel after immersed in free 15% HCl solution; SEM micrograph (c) and EDX analysis (d) of carbon steel after immersed in 15% HCl with 200 ppm of CHOGS-8; SEM micrograph (e) and EDX analysis (f) of carbon steel after immersed in 15% HCl with 200 ppm of CHOGS-16.

CHOGS inhibitors with different chain lengths, the effect of chain length are very important. The difference on the inhibition efficiency in the presence of CHOGS-8, CHOGS-12 and CHOGS-16 in the same concentrations can be justified by the above explanation.

3.10. The relation between surface activity and the corrosion inhibition efficiency of CHOGS compounds

Gemini surfactants have very low critical micelle concentration (CMC) and high solubilising capacity than the corresponding traditional surfactants [63]. It is clear from Table 1 that decreasing CMC values and increasing the hydrophobic chain length of the surfactant molecules increases the inhibition efficiency of the different inhibitors. The highest reduction in surface tension was accomplished with increasing the length of carbon chain of cationic gemini surfactants. This is in good agreement with the inhibition efficiency data which were achieved by investigated surfactants. The obtained values of ΔG^0_{ads} and ΔG^0_{mic}, indicated that the synthesized cationic gemini surfactants favors adsorption rather than micellization. The fact that ΔG^0_{ads} was more negative compared to the corresponding ΔG^0_{mic} could be taken as strong evidence on the formation of strong adsorption film on the steel surface, which matches well with the potentiodynamic and EIS results. It is noticeable that the Γ_{max} values were increased, whilst A_{min} values were decreased with increasing both the corrosion inhibition efficiency and the carbon chain length of CHOGS surfactants. It was evident that, the inhibition efficiency increases with increasing Γ_{max} and π_{CMC} values. All these parameters explain why the synthesized

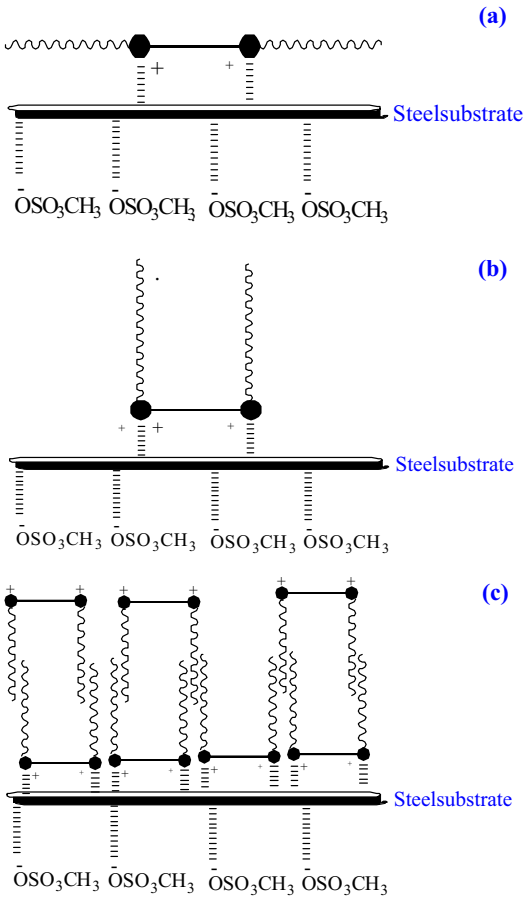

Fig. 12. Mode of adsorption of the synthesized cationic gemini surfactants on the carbon steel substrate in HCl solution.

cationic gemini surfactant was effective inhibitors for carbon steel in 15% HCl.

3.11. Quantum chemical calculation methods

To be able to elucidate the inhibition performance of the investigated gemini surfactants, we scanned the selectivity descriptors and molecular reactivity for these inhibitors. In this study, some quantum calculations were carried out to explain the mode of adsorption of the three studied compounds. The optimized geometry of the gemini surfactants and their HOMO and LUMO distributions are shown in Fig. 13. Table 4 shows some theoretical parameters such as E_{LUMO}, E_{HOMO}, η, σ, χ, ΔN, ΔE, I_P, E_A and μ of the investigated surfactants, which calculated by using Gaussian 09 program package at B3LYP/6-31 G (d, p) level of theory and some related equations.

The quaternary ammonium (N^+) of CHOGS compounds in Fig. 13 exhibited a significant contribution to the HOMO and LUMO distributions. These results suggest that the preferred active sites for electrophilic attack were located within these regions. According to the frontier molecular orbital theory, E_{HOMO} is connected with the ability of molecule to donate the electron to the vacancy d-orbital of steel surface i.e., a molecule with higher E_{HOMO} value is more capable of giving electrons to an acceptor having appropriate vacant molecular orbitals. On the other hand, E_{LUMO} is related to the electron accepting ability of the i.e., lower its value higher would be its electron accepting tendency from the filled metal orbitals [64,65]. Based on EIS and potentiodynamic polarization measurements, the order of inhibition efficiency for the investigated surfactants is CHOGS-16 > CHOGS-12> CHOGS-8. From Table 4, the values of E_{HOMO} for the surfactants CHOGS-16, CHOGS-12 and CHOGS-8 are −6.054, −6.059 and −6.074 eV, respectively. It is well known that in the chemisorption, an increase in E_{HOMO} causes significant increase in inhibition efficiency of inhibitors [66], while the E_{HOMO} negative sign has been explained by some authors to be an indication of physisorption rather than chemisorption [66,67]. Accordingly, the energy gap (ΔE) and the value difference of E_{HOMO} and E_{LUMO} ($\Delta E = E_{LUMO}$-E_{HOMO}) is important parameter in determining the reactivity of a molecule [68,69]. As ΔE decreases, the reactivity of the molecule increases, leading to an increase in adsorption of inhibitor molecules on the steel surface and consequently an increase in the inhibition efficiency. From Table 4, it could be observed that, ΔE values of the three titled surfactants remarkably decrease in the order of CHOGS-8> CHOGS-12 > CHOGS-16, that means the adsorption of studied inhibitors on the metallic surface follows the order CHOGS-16> CHOGS-12 > CHOGS-8.

The dipole moment (μ) is another index that is predominantly utilized for the prediction of the direction of the inhibition of corrosion process. It is related to the distribution of electrons in a molecule and is the measure of polarity in a bond [70]. The compounds with high μ tends to form strong dipole-dipole interactions with the steel surface, leading to resulting in strong adsorption on the metal surface and thence resulting in better *P*% [71]. However, there is no definite correlation between μ and *P*% has been reported in the literature [72]. The data presented in Table 4 indicates that CHOGS-16 has the highest μ and CHOGS-8 has the smallest μ. In our investigation, increasing the μ of the molecules leads to increment their *P*% as a result of increasing the intermolecular forces.

Chemical hardness (η) and softness (σ) are associated with the selectivity and reactivity of the molecule. η measures the resistance of an atom to a charge transfer and μ describes the capacity of an atom or group of atoms to receive electrons. The following equations were used for calculation of η and σ [73]:

$$\eta \cong -\frac{1}{2}(E_{HOMO} - E_{LUMO}) \quad (14)$$

$$\sigma = \frac{1}{\eta} \cong \frac{-2}{(E_{HOMO} - E_{LUMO})} \quad (15)$$

Table 4
Quantum chemical parameters calculated using the Gaussian 09 program package with B3LYP/6–31 G (d, p) basis set for CHOGS models.

Quantum chemical parameters	CHOGS-8 Model	CHOGS-12 Model	CHOGS-16 Model
μ/Debye	1.751	2.946	3.546
E_{HOMO}/eV	−6.074	−6.059	−6.054
E_{LUMO}/eV	0.581	0.472	0.350
ΔE/eV	−6.655	−6.531	−6.404
η/eV	3.3275	3.2655	3.202
σ/eV^{-1}	0.30053	0.30623	0.3123
I_P/eV	6.074	6.059	6.054
E_A/eV	−0.581	−0.472	−0.350
χ/eV	2.7465	2.7935	2.852
ΔN	0.65895	0.6541	0.6457

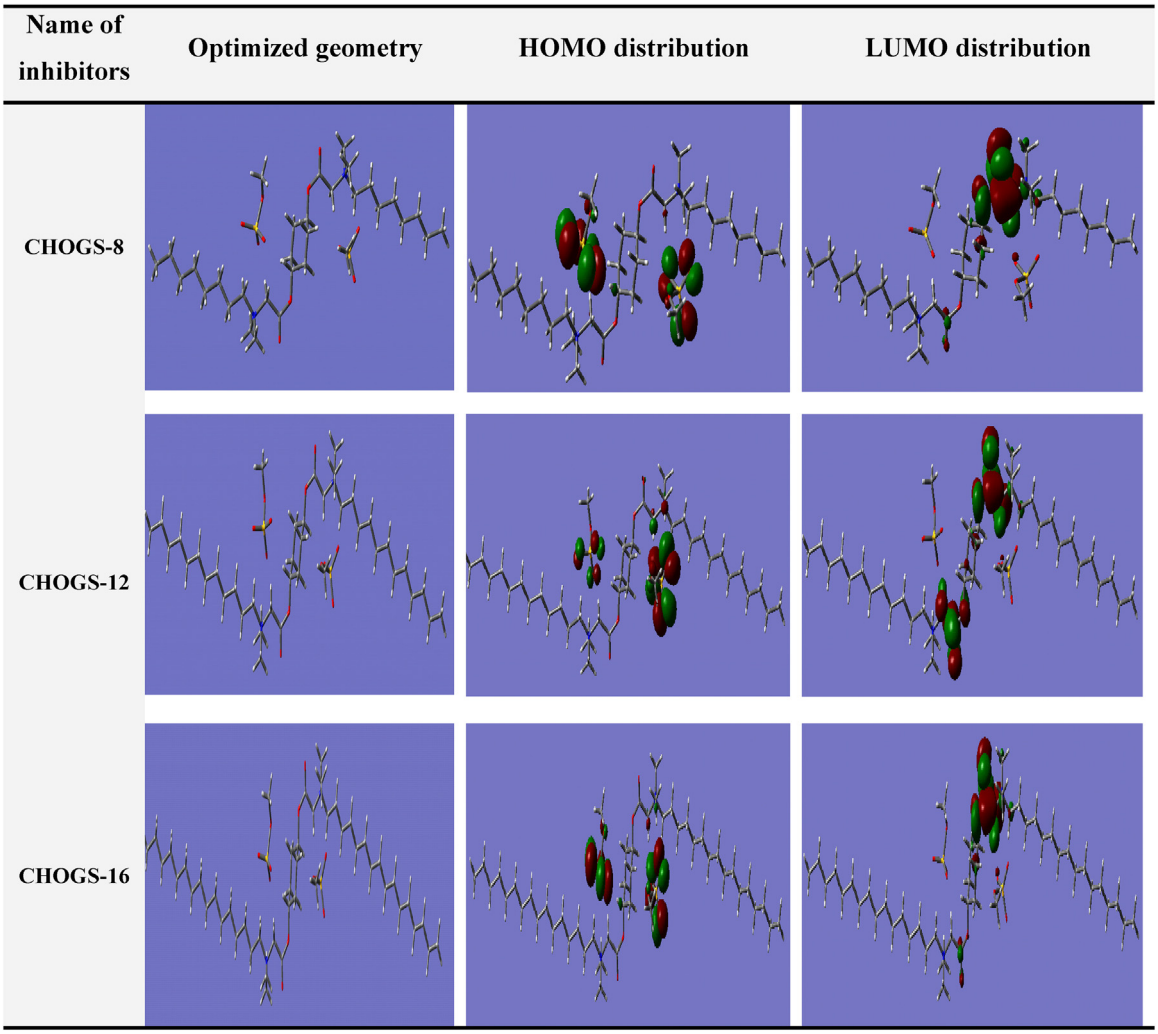

Fig. 13. Optimized structures and frontier molecular orbitals (HOMO and LUMO) for the studied gemini surfactants (a) CHOGS-8, (b) CHOGS-12 and (c) CHOGS-16.

Based on Pearson's hard/soft acids and bases and also the Lewis theory of acid/bases [74], soft molecule would have smaller ΔE and it would be more reactive, and a hard molecule would have larger ΔE value and would be less reactive. A close examination of the values in Table 4 shows that CHOGS-16 has higher σ value, which reveals its softer nature. Thus, CHOGS-16 would have a greater tendency to donate the electrons to the metal. Therefore, the *P*% of the investigated surfactants are CHOGS-16 > CHOGS-12> CHOGS-8, which is in agreement with the empirically obtained results.

Ionization potential (I_p) and electron affinity (E_A) of compounds are measured using Koopmans theorem [75]. Based on this theory the I_p and E_A are related to the E_{HOMO} and E_{LUMO} energies, respectively as follows:

$$I_P = -E_{HOMO} \quad (16)$$

$$E_A = -E_{LUMO} \quad (17)$$

The calculated I_p and E_A results are utilized to obtain the electronegativity (χ) by the following equation [76]:

$$\chi = \frac{I_p + E_A}{2} \quad (18)$$

Pearson method is beneficial in calculating the fraction of electrons (ΔN) transferred from inhibitor to surface of metal [77]. Based on Pearson's method, to calculate the fraction of electron transferred (ΔN), the theoretical value for the absolute electronegativity and hardness of Fe are considered $\chi_{Fe} = 7$ eV and $\eta_{Fe} = 0$, respectively, by considering for metallic bulk $I_p = E_A$ [78]. The ΔN to the Fe-surface can be calculated using the following equation [76]:

$$\Delta N = \frac{\chi_{Fe} - \chi_{inh}}{2(\eta_{Fe} - \eta_{inh})} \quad (19)$$

The ΔN values display the electron transfer from Fe-surface to molecule if $\Delta N < 0$ and molecule to Fe-surface if $\Delta N > 0$ [79]. According to the literature studies, the inhibition efficiency increases with increasing electron-donating capability of the inhibitor at the metallic surface if ΔN less than 3.6 [80]. From Table 4, it could be seen that the ΔN values of the investigated inhibitors are less than 3.6 and positive, indicates that the inhibitor molecules can donate its electrons to metal surface by the formation of coordinate bond. Inspection of data in Table 4 shows that, the ΔN values of the studied inhibitors have very small difference. This confirms the comparable electron donating ability of the investigated surfactant molecules.

The electronegativity (χ) demonstrate electron attracting ability of the inhibitor molecule. The Higher values of χ_{inh} indicate strong attracting power to accept electron from the iron surface. Subsequently, the inhibitor molecules which have higher electronegativity would possess strong interaction with the metallic surface and higher *P*% is observed. According to Table 4, it is observed that the χ_{inh} values of the three studied surfactant molecules obeys the order CHOGS-16 > CHOGS-12 > CHOGS-8.

Thence, it is confirmed that CHOGS-16 has the highest ability to accept electrons among the investigated inhibitor molecules and these results are in well agreement with the empirical findings.

4. Conclusions

New type of cationic gemini surfactants with an ester linkage, is prepared and their performance for carbon steel protection in 15% HCl has been evaluated. The main conclusions are as follow:

1. The synthesized surfactants of CHOGS-8, CHOGS-12 and CHOGS-16 are good corrosion inhibitors for the corrosion of carbon steel in 15% HCl solution. Inhibition efficiency increases with the inhibitor concentration, and the maximum inhibition efficiency at 200 ppm is 97.51% for CHOGS-8; 98.73% for CHOGS-12; and 99.61% for CHOGS-16.
2. The synthesized CHOGS compounds actas mixed-type inhibitors, retarding both cathodic hydrogen evolution reactions and anodic dissolution of metal.
3. The decrease in the C_{dl} andincrease in R_{ct} suggests that the surfactant moleculesfunction by adsorption at the steel/HCl interface.
4. Langmuir adsorption isotherm model described theadsorption of the CHOGS inhibitors utilized in the investigation.
5. The experiments of surface analysis (SEM-EDX)established the adsorption of CHOGS on the carbon steel surface.
6. A close agreement between the surface activity and the corrosion inhibition efficiency was found. Increasing the hydrophobic chain length decreases their surface tension and CMC values and increases their inhibition efficiency.
7. A comparison of the inhibition effectiveness of the synthesized surfactants indicated that their inhibition impacts were closely related to orbital energies (E_{HOMO} and E_{LUMO}), energy gap (ΔE), dipole moment, electronegativity, electron affinity, ionization potential and the fraction of electron transferred.

Acknowledgment

The authors would like to thank **Dr. Kamal Soliman**-Chemistry Department, Faculty of Science, Benha University for his help in quantum chemical calculations.

Appendix A. Supplementary data

Supplementary data associated with this article can be found, in the online version, at http://dx.doi.org/10.1016/j.corsci.2016.03.004

References

[1] H.M. Abd El-Lateef, Synergistic effect of polyethylene glycols and rare earth Ce^{4+} on the corrosion inhibition of carbon steel in sulfuric acid solution: electrochemical, computational, and surface morphology studies, Res. Chem. Intermed. (2015), http://dx.doi.org/10.1007/s11164-015-2207-y (in press).
[2] H.M. Abd El-Lateef, V.M. Abbasov, L.I. Aliyeva, E.E. Qasimov, I.T. Ismayilov, Inhibition of carbon steel corrosion in CO_2-saturated brine using some newly surfactants based on palm oil: experimental and theoretical investigations, Mater. Chem. Phys. 142 (2013) 502–512.
[3] H.M. Abd El-Lateef, A.M. Abu-Dief, B.E.M. El-Gendy, Investigation of adsorption and inhibition effects of some novel anil compounds towards carbon steel in H_2SO_4 solution: electrochemical and theoretical quantum studies, J. Electroanal. Chem. 758 (2015) 135–147.
[4] H.M. Abd El-Lateef, M. Ismael, I.M.A. Mohamed, Novel Schiff base amino acid as corrosion inhibitors for carbon steel in CO_2-saturated 3.5% NaCl solution: experimental and computational study, Corro. Rev. 33 (2015) 77–97.
[5] D.K. Yadav, M.A. Quraishi, Application of some condensed uracils as corrosion inhibitors for mild steel: gravimetric, electrochemical, surface morphological, UV–visible, and theoretical investigations, Ind. Eng. Chem. Res. 51 (2012) 14966–14979.
[6] N. M'hiri, D. Veys-Renaux, E. Rocca, I. Ioannoua, N.M. Boudhriouac, M. Ghoul, Corrosion inhibition of carbon steel in acidic medium by orange peel extract and its main antioxidant compounds, Corros. Sci. 102 (2015) 55–62.
[7] H.M. Abd El-Lateef, Experimental and computational investigation on the corrosion inhibition characteristics of mild steel by some novel synthesized imines in hydrochloric acid solutions, Corros. Sci. 92 (2015) 104–117.
[8] A. Zarrouk, B. Hammouti, A. Dafali, F. Bentiss, Inhibitive properties and adsorption of purpald as a corrosion inhibitor for copper in nitric acid medium, Ind. Eng. Chem. Res. 52 (2013) 2560–2568.
[9] Q. Zhang, Y. Hua, Corrosion inhibition of mild steel by alkylimidazolium ionic liquids in hydrochloric acid, Electrochim. Acta 54 (2009) 1881–1887.
[10] S.T. Keera, M.A. Deyab, Effect of some organic surfactants on the electrochemical behaviour of carbon steel in formation water, Colloids Surf. A: Phys. 266 (2005) 129–140.
[11] G.P. Cicileo, B.M. Rosales, F.E. Varela, J.R. Vilche, Inhibitory action of 8-hydroxyquinoline on the copper corrosion process, Corros. Sci. 40 (1998) 1915–1926.
[12] M. Motamedi, A.R. Tehrani-Bagha, M. Mahdavian, Effect of aging time on corrosion inhibition of cationic surfactant on mild steel in sulfamic acid cleaning solution, Corros. Sci. 70 (2013) 46–54.
[13] L. Niu, H. Zhang, F.H. Wei, S.X. Wu, X.L. Cao, P.P. Liu, Corrosion inhibition of iron in acidic solutions by alkyl quaternary ammonium halides: correlation between inhibition efficiency and molecular structure, Appl. Surf. Sci. 252 (2005) 1634–1642.
[14] M.A. Malik, M.A. Hashim, F. Nabi, S.A. AL-Thabaiti, Z. Khan, Anti-corrosion ability of surfactants: a review, Int. J. Electrochem. Sci. 6 (2011) 1927–1948.
[15] L.G. Qiu, A.J. Xie, Y.H. Shen, Understanding the effect of the spacer length on adsorption of gemini surfactants onto steel surface in acid medium, Appl. Surf. Sci. 246 (2005) 1–5.
[16] A.R. Tehrani-Bagha, K. Holmberg, Cationic ester-containing gemini surfactants: physical–chemical properties, Langmuir 26 (2010) 9276–9282.
[17] Y.-S. Ge, S.-X. Tai, Z.-Q. Xu, L. Lai, F.-F. Tian, D.-W. Li, F.-L. Jiang, Y. Liu, Z.-N. Gao, Synthesis of three novel anionic gemini surfactants and comparative studies of their assemble behavior in the presence of bovine serum albumin, Langmuir 28 (2012) 5913–5920.
[18] L.-H. Zhuang, K.-H. Yu, G.-W. Wangb, C. Yao, Synthesis and properties of novel ester-containing gemini imidazolium surfactants, J. Colloid Interface Sci. 408 (2013) 94–100.
[19] X. Wang, H. Yang, F. Wang, A cationic gemini-surfactant as effective inhibitor for mild steel in HCl solutions, Corros. Sci. 52 (2010) 1268–1276.
[20] M. Mobin, S. Masroor, Cationic gemini surfactants as novel corrosion inhibitor for mild steel in 1.0 M HCl, Int. J. Electrochem. Sci. 7 (2012) 6920–6940.
[21] M.A. Hegazy, Novel cationic surfactant based on triazole as a corrosion inhibitor for carbon steel in phosphoric acid produced by dihydrate wet process, J. Mol. Liq. 208 (2015) 227–236.
[22] B. Xu, W.N. Gong, K.G. Zhang, W.Z. Yang, Y. Liu, X.S. Yin, H. Shi, Y.Z. Chen, Theoretical prediction and experimental study of 1-butyl-2-(4-methylphenyl) benzimidazole as a novel corrosion inhibitor for mild steel in hydrochloric acid, J. Taiwan Inst. Chem. Eng. 51 (2015) 193-.
[23] B. Xu, Y. Liu, X.S. Yin, W.Z. Yang, Y.Z. Chen, Experimental and theoretical study of corrosion inhibition of 3-pyridinecarbozalde thiosemicarbazone for mild steel in hydrochloric acid, Corros. Sci. 74 (2013) 206–213.
[24] K.F. Khaled, M.A. Amin, Dry and wet lab studies for some benzotriazole derivatives as possible corrosion inhibitors for copper in 1.0 M HNO_3, Corros. Sci. 51 (2009) 2098–2106.
[25] H.M. Abd El-Lateef, A.H. Tantawy, Synthesis and evaluation of novel series of schiff base cationic surfactants as corrosion inhibitors for carbon steel in acidic/chloride media: experimental and theoretical investigations, RSC Adv. 6 (2016) 8681–8700.
[26] S.M. Tawffik, Synthesis surface, biological activity and mixed micellar phase properties of some biodegradable gemini cationic surfactants containing oxycarbonyl groups in the lipophilic part, J. Ind. Eng. Chem. 28 (2015) 171–183.
[27] G.H. Sayed, F.M. Ghuiba, M.I. Abdou, E.A. Badr, S.M. Tawfik, N.A. Negm, Synthesis, surface thermodynamic properties of some biodegradable vanillin-Modified polyoxyethylene surfactants, J. Surfact. Deterg. 15 (2012) 735–743.
[28] M.J. Frisch, G.W. Trucks, H.B. Schlegel, G.E. Scuseria, M.A. Robb, J.R. Cheeseman, G. Scalmani, V. Barone, B. Mennucci, G.A. Petersson, H. Nakatsuji, M. Caricato, X. Li, H.P. Hratchian, A.F. Izmaylov, J. Bloino, G. Zheng, J.L. Sonnenberg, M. Hada, M. Ehara, K. Toyota, R. Fukuda, J. Hasegawa, M. Ishida, T. Nakajima, Y. Honda, O. Kitao, H. Nakai, T. Vreven, J.A. MontgomeryJr., J.E. Peralta, F. Ogliaro, M. Bearpark, J.J. Heyd, E. Brothers, K.N. Kudin, V.N. Staroverov, R. Kobayashi, J. Normand, K. Raghavachari, A. Rendell, J.C. Burant, S.S. Iyengar, J. Tomasi, M. Cossi, N. Rega, J.M. Millam, M. Klene, J.E. Knox, J.B. Cross, V. Bakken, C. Adamo, J. Jaramillo, R. Gomperts, R.E. Stratmann, O. Yazyev, A.J. Austin, R. Cammi, C. Pomelli, J.W. Ochterski, R.L. Martin, K. Morokuma, V.G. Zakrzewski, G.A. Voth, P. Salvador, J.J. Dannenberg, S. Dapprich, A.D. Daniels, Ö. Farkas, J.B. Foresman, J.V. Ortiz, J. Cioslowski, D.J. Fox, Gaussian, Inc., Wallingford CT, (2009).
[29] J.E. Del Bene, W.B. Person, K. Szczepaniak, Properties of hydrogen-bonded complexes obtained from the B3LYP functional with 6-31 G (d, p) and 6-31 + G (d, p) basis sets: comparison with MP2/6-31+ G (d, p) results and experimental data, J. Phys. Chem. 99 (27) (1995) 10705–10707.
[30] N.A. Negm, A.M. Al Sabagh, M.A. Migahed, H.M. Abdel Bary, H.M. El Din, Effectiveness of some diquaternary ammonium surfactants as corrosion

inhibitors for carbon steel in 0.5 M HCl solution, Corros. Sci. 52 (2010) 2122–2132.
[31] R. Kamboj, S. Singh, V. Chauhan, Synthesis, characterization and surface properties of *N*-(2-hydroxyalkyl)-*N*-(2-hydroxyethyl) imidazolium surfactants, Colloids Surf. A: Physicochem. Eng. Asp. 441 (2014) 233–241.
[32] R. Zana, Dimeric and oligomeric surfactants. Behavior at interfaces and in aqueous solution: a review, Adv. Colloid Interface Sci. 97 (2002) 205–253.
[33] M.Q. Ao, G.Y. Xu, Y.Y. Zhu, Y. Bai, Synthesis and properties of ionic liquid-type Gemini imidazolium surfactants, J. Colloid Interface Sci. 326 (2008) 490–495.
[34] M.J. Rosen, Surfactants and Interfacial Phenomena, 2nd, Wiley-Interscience, New York, 1989.
[35] Y.R. Hao, X. Yue, X.D. Wang, D.D. Huang, X. Chen, Micelle formation by *N*-alkyl-*N*-methylpiperidinium bromide ionic liquids in aqueous solution, Colloids Surf. A: Physicochem. Eng. Asp. 412 (2012) 90–95.
[36] M.A. Hegazy, A novel Schiff base-based cationic gemini surfactants: synthesis and effect on corrosion inhibition of carbon steel in hydrochloric acid solution, Corros. Sci. 51 (2009) 2610–2618.
[37] L.M. Zhou, X.H. Jiang, Y.T. Li, Z. Chen, X.Q. Hu, Synthesis and properties of a novel class of Gemini pyridinum surfactants, Langmuir 23 (2007) 11404–11408.
[38] M.J. Rosen, Surfactants and Interfacial Phenomena, 3rd edition, John Wiley, New York, 2004.
[39] N.A. Negm, A.F. El Farargy, I.A. Mohammad, M.F. Zaki, M.M. Khowdiary, Synthesis and inhibitory activity of Schiff base surfactants derived from tannic acid and their cobalt (II), manganese (II) and iron (III) complexes against bacteria and fungi, J. Surfact. Deterg. 16 (2013) 767–777.
[40] B. Xu, Y. Ji, X. Zhang, X. Jin, W. Yang, Y. Chen, Experimental and theoretical studies on the corrosion inhibition performance of 4-amino-*N*,*N*-di-(2-pyridylmethyl)-aniline on mild steel in hydrochloric acid, RSC Adv. 5 (2015) 56049–56059.
[41] X. Wang, H. Yang, F. Wang, Inhibition performance of a gemini surfactant and its co-adsorption effect with halides on mild steel in 0.25 M H_2SO_4 solution, Corro. Sci. 55 (2012) 145–152.
[42] T. Gu, Z. Chen, X. Jiang, L. Zhou, Y. Liao, M. Duan, H. Wang, Q. Pu, Synthesis and inhibition of *N*-alkyl-2-(4-hydroxybut-2-ynyl) pyridinium bromide for mild steel in acid solution: Box–Behnken design optimization and mechanism probe, Corros. Sci. 90 (2015) 118–132.
[43] Z. Zhanga, N. Tian, L. Zhang, L. Wu, Inhibition of the corrosion of carbon steel in HCl solution by methionine and its derivatives, Corros. Sci. 98 (2015) 438–449.
[44] A.Y. Musa, A.A.H. Kadhum, A.B. Mohamad, M.S. Takri, Experimental and theoretical study on the inhibition performance of triazole compounds for mild steel corrosion, Corros. Sci. 52 (2010) 3331–3340.
[45] M.A. Hegazy, M. Abdallah, H. Ahmed, Novel cationic gemini surfactants as corrosion inhibitors for carbon steel pipelines, Corro. Sci. 52 (2010) 2897–2904.
[46] M.A. Hegazy, A.S. El-Tabei, A.H. Bedair, M.A. Sadeq, Synthesis and inhibitive performance of novel cationic and gemini surfactants on carbon steel corrosion in 0.5 M H_2SO_4 solution, RSC Adv. 5 (2015) 64633–64650.
[47] B.P. Markhali, R. Naderi, M. Mahdavian, M. Sayebani, S.Y. Arman, Electrochemical impedance spectroscopy and electrochemical noise measurements as tools to evaluate corrosion inhibition of azole compounds on stainless steel in acidic media, Corros. Sci. 75 (2013) 269–279.
[48] T. Pajkossy, Impedance of rough capacitive electrodes, J. Electroanal. Chem. 364 (1994) 111–125.
[49] B. Xu, W.Z. Yang, Y. Liu, X.S. Yin, W.N. Gong, Y.Z. Chen, Experimental and theoretical evaluation of two pyridinecarboxaldehyde thiosemicarbazone compounds as corrosion inhibitors for mild steel in hydrochloric acid solution, Corros. Sci. 78 (2014) 260–268.
[50] Z.Y. Cao, Y.M. Tang, H. Cang, J.Q. Xu, G. Lu, W.H. Jing, Novel benzimidazole derivatives as corrosion inhibitors of mild steel in the acidic media. Part II: theoretical studies, Corros. Sci. 83 (2014) 292–298.
[51] M.A. Chidiebere, E.E. Oguzie, L. Liu, Y. Li, F. Wang, Corrosion inhibition of Q235 mild steel in 0.5 M H_2SO_4 solution by phytic acid and synergistic iodide additives, Ind. Eng. Chem. Res. 53 (2014) 7670–7679.
[52] D.K. Yadav, M.A. Quraishi, B. Maiti, Inhibition effect of some benzylidenes on mild steel in 1 M HCl: an experimental and theoretical correlation, Corros. Sci. 55 (2012) 254–266.
[53] V.V. Torres, V.A. Rayol, M. Magalhães, G.M. Viana, L.C.S. Aguiar, S.P. Machado, H. Orofino, E. D'Elia, Study of thioureas derivatives synthesized from a green route as corrosion inhibitors for mild steel in HCl solution, Corros. Sci. 79 (2014) 108–118.
[54] P.C. Okafor, Y. Zheng, Synergistic inhibition behavior of methylbenzyl quaternary imidazoline derivative and iodide ions on mild steel in H_2SO_4 solutions, Corros. Sci. 51 (2009) 850–859.
[55] D. Asefi, M. Arami, A.A. Sarabi, N.M. Mahmoodi, The chain length influence of cationic surfactant and role of nonionic co-surfactants on controlling the corrosion rate of steel in acidic media, Corros. Sci. 51 (2009) 1817–1821.
[56] K. Khaled, Corrosion control of copper in nitric acid solutions using some amino acids—a combined experimental and theoretical study, Corros. Sci. 52 (2010) 3225–3234.
[57] S.H. Yoo, Y.W. Kim, K. Chung, N.K. Kim, J.-S. Kim, Corrosion inhibition properties of triazine derivatives containing carboxylic acid and amine groups in 1.0 M HCl solution, Ind. Eng. Chem. Res. 52 (2013) 10880–10889.
[58] H.M. Abd El-Lateef, A.M. Abu-Dief, L.H. Abdel-Rahman, E.C. Sañudo, N. Aliaga-Alcalde, Electrochemical and theoretical quantum approaches on the inhibition of C1018 carbon steel corrosion in acidic medium containing chloride using some newly synthesized phenolic Schiff bases compounds, J. Electroanal. Chem. 743 (2015) 120–133.
[59] M. Behpour, S.M. Ghoreishi, N. Soltani, M. Salavati-Niasari, M. Hamadanian, A. Gandomi, Electrochemical and theoretical investigation on the corrosion inhibition of mild steel by thiosalicylaldehyde derivatives in hydrochloric acid solution, Corros. Sci. 50 (2008) 2172–2181.
[60] M.A. Hegazy, M. Abdallah, M.K. Awad, M. Rezk, Three novel di-quaternary ammonium salts as corrosion inhibitors for API X65 steel pipeline in acidic solution Part I: Experimental results, Corros. Sci. 81 (2014) 54–64.
[61] R. Solmaz, G. Kardas, B. Yazıcı, M. Erbil, Adsorption and corrosion inhibitive properties of 2-amino-5-mercapto-1,3,4-thiadiazole on mild steel in hydrochloric acid media, Colloids Surf. A: Physicochem. Eng. Aspects 312 (2008) 7–17.
[62] D. Asefi, N.M. Mahmoodi, M. Arami, Effect of nonionic co-surfactants on corrosion inhibition effect of cationic gemini surfactant in acid medium, Colloids Surf. A 355 (2010) 183–186.
[63] M.A. Malik, M.A. Hashim, F. Nabi, S.A. AL-Thabaiti, Z. Khan, Anti-corrosion ability of surfactants: a review, Int. J. Electrochem. Sci. 6 (2011) 1927–1948.
[64] M. Yadav, L. Gope, N. Kumari, P. Yadav, Corrosion inhibition performance of pyranopyrazole derivatives for mild steel in HCl solution: gravimetric, electrochemical and DFT studies, J. Mol. Liq. 216 (2016) 78–86.
[65] S. Zor, M. Saracoglu, F. Kandemirli, T. Arslan, Inhibition effects of amides on the corrosion of copper in 1.0 M HCl: theoretical and experimental studies, Corrosion 67 (2011) 125003-1–125003-11.
[66] A. Aytaç, S. Bilgiç, G. Gece, N. Ancın, S.G. Öztaş, Experimental and theoretical study of the inhibition effects of some Schiff bases as corrosion inhibitors of aluminium in HCl, Mater. Corros. 62 (2011) 9999.
[67] N.K. Allam, Thermodynamic and quantum chemistry characterization of the adsorption of triazole derivatives during muntz corrosion in acidic and neutral solutions, Appl. Surf. Sci. 253 (2007) 4570–4577.
[68] S. Xia, M. Qiu, L. Yu, F. Liu, H. Zhao, Molecular dynamics and density functional theory study on relationship between structure of imidazoline derivatives and inhibition performance, Corros. Sci. 50 (2008) 2021–2029.
[69] L. Feng, H. Yang, F. Wang, Experimental and theoretical studies for corrosion inhibition of carbon steel by imidazoline derivative in 5% NaCl saturated Ca $(OH)_2$ solution, Electrochim. Acta 58 (2011) 427–436.
[70] I.B. Obot, N.O. Obi-Egbedi, Indeno-1-one [2,3-b] quinoxaline as an effective inhibitor for the corrosion of mild steel in 0.5 M H_2SO_4 solution, Mater. Chem. Phys. 122 (2010) 325–328.
[71] B.D. Mert, M.E. Mert, M.E. Kardas, G. Yazici, Experimental and theoretical investigation of 3-amino-1 2, 4-triazole-5-thiol as a corrosion inhibitor for carbon steel in HCl medium, Corros. Sci. 53 (2011) 4265–4272.
[72] G. Gece, The use of quantum chemical methods in corrosion inhibitor studies, Corros. Sci. 50 (2008) 2981–2992.
[73] L.C. Murulana, M.M. Kabanda, E.E. Ebenso, Experimental and theoretical studies on the corrosion inhibition of mild steel by some sulphonamides in aqueous HCl, RSC Adv. 5 (2015) 28743–28761.
[74] I.B. Obot, D.D. Macdonald, Z.M. Gasem, Density functional theory (DFT) as a powerful tool for designing new organic corrosion inhibitors. Part 1: an overview, Corros. Sci. 99 (2015) 1–30.
[75] A. Dutta, S. Kr Saha, P. Banerjee, D. Sukul, Correlating electronic structure with corrosion inhibition potentiality of some bis-benzimidazole derivatives for mild steel in hydrochloric acid: combined experimental and theoretical studies, Corros. Sci. 98 (2015) 541–550.
[76] S. Kr Saha, A. Dutta, P. Ghosh, D. Sukul, P. Banerjee, Adsorption and corrosion inhibition effect of Schiff base molecules on the mild steel surface in 1 M HCl medium: a combined experimental and theoretical approach, Phys. Chem. Chem. Phys. 17 (2015) 5679–5690.
[77] S. Martinez, Inhibitory mechanism of mimosa tannin using molecular modeling and substitutional adsorption isotherms, Chem. Phys. 77 (2002) 97–102.
[78] M.J.S. Dewar, W. Thiel, the MNDO method approximations and parameters, J. Am. Chem. Soc. 99 (1977) 4899–4907.
[79] A. Kokalj, Is the analysis of molecular electronic structure of corrosion inhibitors sufficient to predict the trend of their inhibition performance, Electrochim. Acta 56 (2010) 745–755.
[80] M.K. Awad, M.R. Mustafa, M.M.A. Elnga, Computational simulation of the molecular structure of some triazoles as inhibitors for the corrosion of metal surface, J. Mole. Struct. (Theochem) 959 (2010) 66–74.